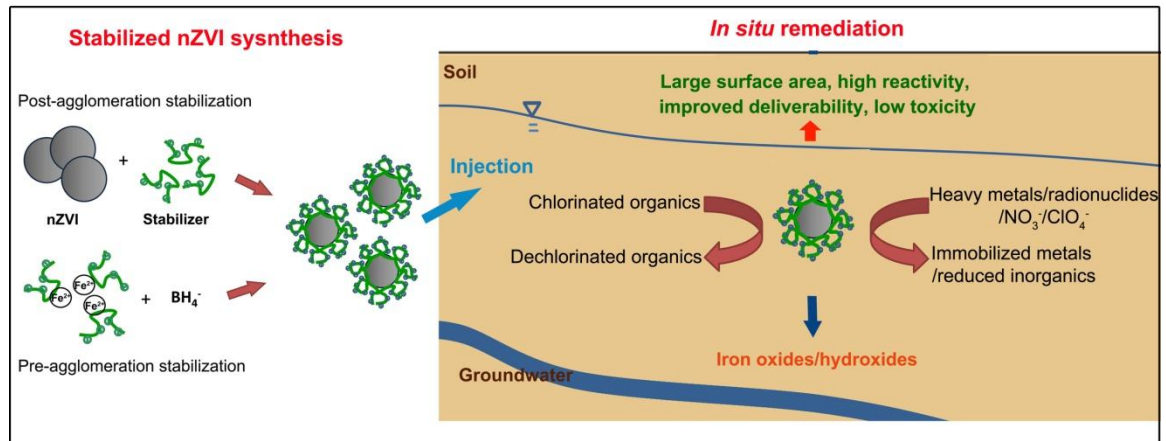


## Graphical abstract



**An overview of preparation and applications of stabilized zero-valent iron  
nanoparticles for soil and groundwater remediation**

Xiao Zhao<sup>a,1</sup>, Wen Liu<sup>a,1</sup>, Zhengqing Cai<sup>a</sup>, Bing Han<sup>a</sup>, Tianwei Qian<sup>b</sup>, Dongye Zhao<sup>a,b,\*</sup>

<sup>a</sup>Environmental Engineering Program, Department of Civil Engineering, Auburn University,  
Auburn, AL 36849, USA

<sup>b</sup>Institute of Environmental Science, Taiyuan University of Science and Technology, Taiyuan,  
Shanxi 030024, PR China

<sup>1</sup> Equal contributions.

\*Corresponding author. Phone: +1 334-844-6277; Fax: +1 334-844-6290;

E-mail: zhaodon@auburn.edu

## Contents

<b>List of abbreviation.....</b>	<b>3</b>
<b>Abstract.....</b>	<b>5</b>
<b>1. Introduction.....</b>	<b>6</b>
<b>2. Evolution of nZVI-based technology and preparation of stabilized nZVI.....</b>	<b>9</b>
2.1. A brief history on the evolution of ZVI-based cleanup technology .....	9
2.2. Preparation of non-stabilized ZVI particles .....	12
2.3. Preparation of stabilized nZVI.....	13
<b>3. Applications of stabilized nZVI for environmental remediation .....</b>	<b>25</b>
3.1. Applications of stabilized nZVI for transformation of organic contaminants .....	26
3.2. Applications of stabilized nZVI for removal/immobilization of inorganic contaminants .....	29
3.3. Field studies on application of stabilized nZVI for <i>in situ</i> remediation .....	34
3.4. Factors affecting properties and effectiveness of stabilized nZVI.....	37
<b>4. Transport of stabilized nZVI .....</b>	<b>40</b>
<b>5. Fate and toxicity of stabilized nZVI.....</b>	<b>44</b>
<b>6. <i>In situ</i> remediation using stabilized nZVI: merits and limitations.....</b>	<b>49</b>
<b>7. Technical constraints and future research needs.....</b>	<b>50</b>
<b>8. Conclusions.....</b>	<b>52</b>
<b>Acknowledgments .....</b>	<b>53</b>
<b>References.....</b>	<b>53</b>

## 42 **List of abbreviation**

43	CMC	Carboxymethyl cellulose
44	CSC	Critical stabilization concentration
45	CTAB	Cetyltrimethyl-ammonium bromide
46	CVOCs	Chlorinated volatile organic compounds
47	DCA	Dichloroethane
48	DCE	Dichloroethene
49	DNAPLs	Dense non-aqueous phase liquids
50	DO	Dissolved oxygen
51	DOE	Department of Energy
52	DOM	Dissolved organic matter
53	EDTA	Ethylenediamine tetraacetic acid
54	ID	Inner diameter
55	IW	Injection well
56	MW	Monitoring well
57	M.W.	Molecular weight
58	NASA	National Aeronautics and Space Administration
59	NOM	Natural organic matter
60	OMA	Olefin maleic acid
61	PAA	Poly(acrylic acid)
62	PAM	Polyacrylamide
63	PAP	Polyaspartate
64	PBET	Physiologically based extraction test
65	PCE	Perchloroethylene
66	PCBs	Polychlorinated biphenyls
67	PMAA-PMMA-PSS	Poly(methacrylic acid)-block-(methyl methacrylate or butyl
68		methacrylate)-block-(styrenesulfonate)
69	PRB	Permeable reactive barrier

70	PSS	Poly styrene sulfonate
71	PV	Pore volume
72	PVP	Polyvinylpyrrolidone
73	PV3A	Polyvinyl alcohol-co-vinyl acetate-co-itaconic acid
74	ROS	Reactive oxygen species
75	SDBS	Dodecylbenzene-sulfonic acid, sodium salt
76	SOM	Soil organic matter
77	TCA	Trichloroethane
78	TCE	Trichloroethylene
79	TCLP	Toxicity characteristic leaching procedure
80	TEM	Transmission electron microscope
81	VC	Vinyl chloride
82	wt%	Weight%
83	XG	Xanthan gum
84	ZVI	Zero-valent iron
85	nZVI	Nano-scale zero-valent iron

86

87

88

89

90

91

92

93

94

95

## Abstract

Nano-scale zero-valent iron (nZVI) is one of the most intensively studied materials for environmental cleanup uses over the past 20 years or so. Freshly prepared nZVI is highly reactive due to its high specific surface area and strong reducing power. Over years, the classic borohydride reduction method for preparing nZVI has been modified by use of various stabilizers or surface modifiers to acquire more stable and soil deliverable nZVI for treatment of different organic and inorganic contaminants in water and soil. While most studies have been focused on testing nZVI for water treatment, the greater potential or advantage of nZVI appears to be for *in situ* remediation of contaminated soil and groundwater by directly delivering stabilized nZVI into the contaminated subsurface as it was proposed from the beginning. Compared to conventional remediation practices, the *in situ* remediation technique using stabilized nZVI offers some unique advantages. This work provides an update on the latest development of stabilized nZVI for various environmental cleanup uses, and overviews the evolution and environmental applications of stabilized nZVI. Commonly used stabilizers are compared and the stabilizing mechanisms are discussed. The effectiveness and constraints of the nZVI-based *in situ* remediation technology are summarized. This review also reveals some critical knowledge gaps and research needs, such as interactions between delivered nZVI and the local biogeochemical conditions.

**Keywords:** Stabilized nanoparticles; Zero-valent iron; Soil remediation; Groundwater; Water contamination; Dechlorination

## 1. Introduction

Iron is the most abundant transition metal and the fourth most plentiful element in the Earth crust (Huber, 2005). Accordingly, various iron-containing materials have been intensively studied in different natural and engineered environmental processes. Zero-valent iron (ZVI) has been widely investigated for environmental remediation due to its fairly strong reducing power ( $E_0 = -0.44$  V) and its ability to adsorb an array of important contaminants such as heavy metals and metalloids. The earliest environmental uses of ZVI were on reductive dechlorination of chlorinated solvents. For example, Gillham and O'Hannesin (1994) reported that iron filings were able to reduce a number of halogenated aliphatic compounds.

Nano-scale zero-valent iron (nZVI) materials have been found more reactive than conventional iron powder or iron filings because of the greater specific surface area and possibly the nano-scale effects. Although most published works have been devoted to treatment of organic and inorganic contaminants in water, the most unique and promising environmental application of nZVI-based technology is believed to be for *in situ* remediation of contaminated soil and groundwater as it was proposed in the beginning (Wang and Zhang, 1997), in particular, for aquifers that are difficult to reach by conventional technologies.

*In situ* remediation of soil and groundwater by directly delivering nZVI into the contaminated source zones had been studied at about 70 pilot and full-scale field sites by 2015 (Bardos et al., 2015). Fig. 1 presents a schematic of an *in situ* remediation technology for reductive dechlorination of chlorinated solvents, such as trichloroethylene (TCE) and polychlorinated biphenyls (PCBs) by injecting stabilized ZVI nanoparticles into a contaminated source zone. Compared to conventional remediation practices, the *in situ* remediation technique using stabilized nZVI offers some unique advantages, including 1) it can reach contaminants in

deep aquifers or in areas not accessible by other methods, 2) it can proactively attack contaminant plumes in source zones, 3) it is less destructive, and 4) it is likely much more cost-effective and less time-consuming (EPA, 2004; Karn et al., 2009; Piquepaille, 2003).

**[Fig. 1]**

For the process to be successful, several key criteria will have to be met. First, the nanoparticles will have to be deliverable in the soil or other geo-media; second, the delivered nanoparticles will provide sufficient reactivity toward the target contaminants; third, the nanoparticles will be able to effectively “meet” with the contaminants to initiate the reaction; and fourth, the delivered nanoparticles will not cause adverse effects on the local environmental conditions. Due to the natural filtration effect of soil and strong aggregation of ZVI nanoparticles, the most prominent technical obstacle has been soil mobility or deliverability (He and Zhao, 2005).

Traditionally, nZVI particles are prepared through the bottom-up methods such as the aqueous-phase borohydride reduction approach (Corrias et al., 1990; Glavee et al., 1995; Wang and Zhang, 1997), micro-emulsion-based methods (Li et al., 2003), sonication assisted methods and sol-gel methods (Suslick et al., 1996; van Wonterghem et al., 1985), of which the aqueous borohydride reduction method has been most widely used because of the minimal use of environmentally intensive solvents or chemicals. Commercial nZVI is available from several sources (e.g., Toda Kogyo Ltd. (Japan), Nano Iron (Czech Republic), Golder Associates Inc. (USA)). Generally, the industrial nZVI is produced by thermal reduction of iron oxide precursors with hydrogen gas or through ball-milling (Li et al., 2009). Due to the extremely large area-to-volume ratio, magnetic attraction, and the high surface energy and reactivity, ZVI nanoparticles tend to aggregate rapidly into micro to millimeter scale flocs. In addition, the highly reactive



nanoparticles react with the surrounding media, such as dissolved oxygen (DO) and water, losing their reactivity. Mondal et al. (2004) reported that because of agglomeration, the mean particle size of the “nanoparticles” is actually ~17.7  $\mu\text{m}$ . Because particles of 3  $\mu\text{m}$  or larger are easily intercepted by soil matrix (Schrick et al., 2004), the agglomerated iron particles are not deliverable in soil.

To prevent particle aggregation and facilitate soil delivery, various surface modification or stabilization techniques have been investigated over the last 15 years or so. Typically, polymeric molecules are coated on the particles. These coated macromolecules act as a barrier to prevent particle aggregation through electrostatic and/or steric repulsion. Compared to aggregated particles, stabilized nanoparticles offer a number of key advantages, including 1) while non-stabilized nanoparticles agglomerate rapidly, stabilized nanoparticles remain in the nanoscale, and thus are deliverable or transportable in soil or sediment; 2) stabilized nanoparticles may offer greater reactivity than non-stabilized counterparts, leading to more effective and complete dechlorination (less or no intermediate toxins produced); 3) the use of stabilizers of different physical and chemical characteristics (e.g., molecular weight, matrix type, functionality, degree of substitution, and viscosity) may facilitate control of physical dispersibility, chemical reactivity and reactive longevity of stabilized nanoparticles.

Laboratory and field studies have demonstrated that stabilized nZVI particles can effectively degrade halogenated organics, and immobilize toxic metals, metalloids and radionuclides (He and Zhao, 2005, 2007, 2008; He et al., 2007, 2009a, 2009b, 2010; Liu et al., 2015; Xu and Zhao, 2007). However, because of the complexity of the soil physical and biogeochemical properties, the effectiveness and feasibility of the *in situ* remediation technology using stabilized nZVI are yet to be further studied, especially at the field scale (Liu et al., 2015). The technology

constraints and environmental factors that affect the particle reactivity, mobility and environmental fate are yet to be determined or confirmed under field conditions. Several recent review papers summarized the important developments and perspectives of non-stabilized ZVI (e.g., Crane and Scott, 2012; Yan et al., 2013; Fu et al., 2014; Guan et al., 2015), yet a thorough overview of stabilized/modified nZVI has been missing. Table 1 summarizes some of recent important reviews on nZVI.

#### **[Table 1]**

The objectives of this review were to: 1) update the latest development on synthesis of stabilized nZVI, 2) examine factors that influence the reactivity and properties of stabilized nZVI, 3) overview the environmental applications of stabilized nZVI, 4) evaluate the fate and transport of stabilized nZVI in the environment, and 5) identify knowledge gaps and future research needs. It is noted that traditional iron powder or filings without stabilizers are not in the nanoscale and not suitable for *in situ* delivery into soil, and thus, are excluded from this review.

## **2. Evolution of nZVI-based technology and preparation of stabilized nZVI**

### **2.1. A brief history on the evolution of ZVI-based cleanup technology**

From iron powder/filings, to non-stabilized nZVI and stabilized nZVI, nZVI-based remediation of soil and groundwater has come a long way over the last 25 years or so. Fig. 2 provides a chronicle overview of the major milestones on the evolution and environmental uses of the technology. The development of nZVI-based remediation technology may be split into the following stages: 1) synthesis and characterization of bare or non-stabilized ZVI, which are essentially ZVI aggregates with some primary particles being in the nanoscale, 2) reductive dechlorination of chlorinated solvents (e.g., TCE and PCBs) and adsorption of inorganic

contaminants (e.g., metals) in the aqueous phase using non-stabilized ZVI particles, 3) synthesis, characterization and testing of stabilized nZVI for reductive dechlorination and reductive immobilization of redox-active metals and radionuclides, and 4) studies on environmental fate, transport and toxicity of bare and stabilized nZVI.

**[Fig. 2]**

Conventionally, non-stabilized ZVI is prepared by reduction of  $\text{Fe}^{2+}/\text{Fe}^{3+}$  ions using borohydride ( $\text{BH}_4^-$ ) in the aqueous phase. The earliest study on this method can be dated back to 1953, when Schlesinger et al. (1953) used borohydride to reduce a number of transition metal ions including  $\text{Fe}^{2+}$  to promote hydrogen production. Later, Brown and Brown (1962) confirmed that borohydride was able to reduce a host of platinum family metals including  $\text{Fe}^{2+}$  to the elemental state. Yet, detailed studies on the chemistry were not reported until 1990 by Corrias et al. (1990) and then 1995 by Glavee et al. (1995), who were the first to determine the size of synthesized powder and started to use the term “nanoscale Fe powder”.

The earliest environmental use of ZVI was reported by Gould (1982), who studied reduction kinetics of hexavalent chromium by metallic iron wire. Later, Senzaki (1988) and Senzaki and Kumagai (1988a, 1988b, 1991) observed that iron powder can effectively reduce chlorinated organic compounds in wastewater. The first field study of granular ZVI was carried out in 1991 where ZVI was used in a permeable reactive barrier (PRB) for *in situ* remediation of groundwater contaminated by TCE and PCE at a Canadian site (Guan et al., 2015; O'Hannesin and Gillham, 1992). The success triggered rapid increase in ZVI uses in PRBs. By 2003, ~70 PRBs employed commercial granular iron to degrade chlorinated hydrocarbons (Gillham, 2003).

Gillham (1993), Gillham and O'hannesin (1994), and Matheson and Tratnyek (1994) pioneered more systematic studies on ZVI for dechlorination uses, which essentially opened up a long-lasting research area. The authors reported that ZVI fillings or electrolytic iron powder can effectively dechlorinate chlorinated organic compounds in groundwater. Matheson and Tratnyek (1994) also illustrated the fundamental chemistry on the iron corrosion and dehalogenation pathways, and for the first time, they showed that increasing the clean surface area of iron greatly increased the rate of carbon tetrachloride dehalogenation. Later, Agrawal and Tratnyek (1995) reported that iron powder was also able to reduce nitro aromatic compounds. Johnson et al. (1996) carried out a detailed study on kinetics of ZVI-mediated dehalogenation and compared the dechlorination rates by iron powders from 18 sources. The study revealed the reaction rates obtained from different sources correlate positively with the reactive surface area.

The concept of *in situ* dechlorination in the subsurface using nZVI was first conceived by Wang and Zhang (1997), who postulated that nZVI may be directly injected into the contaminated subsurface and facilitate *in situ* remediation of contaminated soil and groundwater (Zhang, 2003). Wang and Zhang (1997) demonstrated the effectiveness of synthetic, non-stabilized ZVI particles for reductive dechlorination, and noted that the freshly prepared ZVI particles are much more reactive than commercial iron powders. Zhang et al. (1998) also reported that adding a small fraction of a catalyst (Pd) increased the surface-area-normalized rate constant by ~100 times. Because of the tremendous impacts of chlorinated hydrocarbons in soils, this concept enticed immediate and broad research interests. However, all these pioneering works were carried out in aqueous solutions, and did not address other critical issues related to soil remediation, such as particle aggregation and soil deliverability. Subsequently, the technology

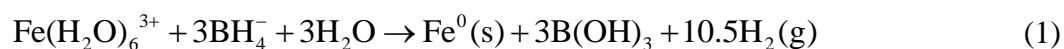
stepped into a new stage that highlighted particle stabilization and soil transportability (Schrick et al., 2004; He and Zhao, 2005; He et al., 2007).

## 2.2. Preparation of non-stabilized ZVI particles

Generally, three major techniques have been used to obtain bare ZVI particles, including 1) top-down methods, such as the high energy ball milling of bulk iron particles, 2) bottom-up methods, i.e., aqueous-phase reduction of  $\text{Fe}^{2+}/\text{Fe}^{3+}$ , and 3) gas-phase reduction of iron oxides to ZVI via hydrogen gas or some other scalable approaches.

Li et al. (2009) obtained ZVI particles by ball-milling commercial iron powder (mean size = 2  $\mu\text{m}$ ). Upon half-hour milling, the material acquired a specific surface area of 5.5  $\text{m}^2 \text{g}^{-1}$  and a mean diameter of 140 nm (primary particles in the form of aggregates). Further milling for 8 hours increased the surface area to 39  $\text{m}^2 \text{g}^{-1}$  and reduced the size to 40–60 nm. The resulting ZVI offered comparable reactivity with that prepared through the aqueous borohydride reduction, and the ball milling method was claimed less energy-intensive and less time-consuming for large-scale production (Li et al., 2009). However, the particles aggregate in water rapidly into micron-scale or larger particles, which are hardly deliverable in soil.

Bottom-up methods have been commonly used in most studies. Most commonly, nZVI is synthesized by reduction of ferrous or ferric ions in aqueous solutions using sodium borohydride under inert conditions per reactions (He and Zhao, 2005, 2007; Wang and Zhang, 1997):



Sodium borohydride is a strong reducing agent, and has been used for preparation of amorphous alloy particles for more than half-century (Vanwonterghem et al., 1986). Yet, its high cost is the major concern for the wet chemical synthesis of nZVI. The estimated cost for borohydride reduced nZVI is over \$200/kg (Yan et al., 2013).

In search for a cheaper and “greener” reducing agent, some organic reducing agents have been employed in synthesis of ZVI particles, where the organics may also serve as capping agents. For example, well capped nZVI particles were obtained using polyphenolic compounds from tea leaves (Hoag et al., 2009) and sorghum bran extracts (Njagi et al., 2011) as the reducing agents. The size and morphology of the resulting nZVI were dependent on the concentration of the extracts. The findings led to the concept that nZVI may be formed *in situ* by injecting the reductants into the subsurface where dissolved  $\text{Fe}^{2+}/\text{Fe}^{3+}$  ions are available. However, the nZVI yield is dependent upon the available iron precursors, among other factors, and the reactivity of nZVI produced in this manner was lower than that by the borohydride method (Hoag et al., 2009).

The cost of commercially available nano-scale ZVI is much higher than conventional powder or granular ZVI. Crane and Scott (2012) reported that the price of commercial nZVI in 2012 ranged from £50 to £150 per kg (~\$80 to 238\$ per kg) compared to less than £1/kg (~\$ 1.6/kg) for granular iron. Bardos et al. (2015) estimated the cost of nZVI in the U.S. ranged from \$66 to \$88 per kg, compared to \$2 to \$11 per kg for micro-scale ZVI.

## **2.3. Preparation of stabilized nZVI**

### **2.3.1. Mechanisms of particle aggregation and stabilization.**

Agglomeration of metal nanoparticles is a thermodynamically favorable process, and it can take place in a number of fashions, including: 1) Ostwald ripening (i.e. during particle formation and growth, particles smaller than the critical size will dissolve, and then taken by the larger particles), 2) arrested precipitation (precipitation facilitated by formation of nucleation centers), and 3) direct inter-particle interactions (He and Zhao, 2005, 2007; Laurent et al., 2008; Sun and Zeng, 2002). The inter-particle forces may include van der Waals forces, magnetic dipolar interactions, and electric dipolar interactions. Particle agglomeration renders the particles undeliverable in soil, and reduces the specific surface area, thereby diminishing particle reactivity. The reductive reactivity can also be weakened due to reaction with water. Therefore, the key to stabilize nZVI nanoparticles is to control the inter-particle interactions and particle growth, and to passivate the particle surface from being reacted “too quickly” by the media.

In the past decade or so, several stabilization techniques have been investigated and compared for their effects on nZVI dispersibility and stability. Generally, stabilization of nZVI can be realized through surface modification and/or creating a network that separates the nanoparticles as depicted in Fig. 3. In the surface modification method, stabilizer molecules are attached onto the nZVI surface to create or enhance repulsive forces including electrostatic double layer repulsion, osmotic repulsion or electrosteric repulsion; in the network stabilization, a stabilizer is added at high doses to facilitate formation of a viscous or gel matrix/network through hydrogen bonding and polymer entanglements (Comba and Sethi, 2009), thereby preventing particle aggregation. Two different scenarios can exist in network stabilization (Fig. 3): 1) stabilizers are attached onto nZVI and integrate nZVI within the gel structure, and b) the non-adsorbing stabilizers generates a network around nZVI to separate them from each other. As a result, the frequency of collisions between nanoparticles can be greatly reduced due to the

stiffness of the stabilizer matrix/network where nanoparticles are trapped (Comba and Sethi, 2009; Tosco et al., 2014).

### **[Fig. 3]**

In summary, a stabilizer enhances dispersion of nanoparticles through: 1) electrostatic stabilization (adsorption of charged stabilizer molecules to the core metal, which creates an electrical double layer and results in Coulombic repulsion between the stabilizer-capped particles), 2) steric stabilization (coating the metal core with macromolecular stabilizers such as polymers impedes particle attractions through the osmotic repulsive force, which arises when the layers of stabilizer molecules overlap), 3) electrosteric stabilization (through combined electrostatic and steric interactions), and 4) network stabilization (or viscous stabilization). As a rule, macromolecules of larger molecular weight and high densities of charged functional groups are more effective stabilizers. In addition to enhanced dispersibility of nanoparticles, coating a stabilizer onto nanoparticles may also passivate the reactive particle surface from being reacted with the media (e.g. H<sub>2</sub>O and DO).

### **2.3.2. Stabilization of nZVI using various stabilizers**

A great deal of effort has been devoted to “stabilizing” or capping various metal nanoparticles. In general, stabilizing nZVI is more difficult than metal oxide or noble-metal nanoparticles (e.g. Au and Ag) because of the high surface reactivity and the strong inter-particle interactions (van der Waals and magnetic interactions). To prevent iron particles and iron oxide nanoparticles from agglomeration, various stabilizers have been found effective, including thiols, carboxylic acids, silica, surfactants, polymers, water soluble polysaccharides, poly (acrylic acids), styrenesulfonic acids, vinylsulfonic acid, and long chain alcohols (Chatterjee et al., 2002; Lin et



al., 2005; Saleh et al., 2005; Mykhaylyk et al., 2001; Pardoe et al., 2001; Wang and Zhang, 1997; Xu and Bhattacharyya, 2005). Obviously, not all these stabilizers are applicable to nZVI. For example, some polymers may not function properly in water (Kim et al., 2003a), and some of the stabilizers may cause secondary contamination when introduced into the subsurface.

Particle stabilization can be carried out in two ways: 1) pre-agglomeration stabilization, i.e. adding a stabilizer before aggregates are formed, or during the growth of nanoparticles; and 2) post-agglomeration stabilization, where a stabilizer is applied to disperse or emulsify the formed nZVI aggregates. For the latter, sonication treatment is often exercised to break down the aggregates during or before a stabilizer is added. For instance, commercial nZVI powder obtained by thermal H<sub>2</sub> reduction may be dispersed into an aqueous solution through post-agglomeration stabilization. Compared to bare nZVI, nZVI synthesized following the pre-agglomeration stabilization appeared more reactive when used for TCE dechlorination (Cho and Choi, 2010; He and Zhao, 2008), while nZVI prepared *via* the post-agglomeration stabilization appeared less reactive (Phenrat et al., 2009). Thermodynamically, the pre-agglomeration stabilization is more favorable and likely to obtain smaller particles, while the post-agglomeration stabilization is often limited by the ability to break down the already formed aggregates. In addition, the additional treatment to break down the aggregation may also induce corrosion of ZVI and the polymer molecules are more likely to block the reactive sites as more stabilizers are often needed compared to pre-aggregation method, both resulting in significant reactivity loss (Tratnyek et al., 2011).

The stabilizers for nZVI stabilization may be categorized into the following groups: a) surfactants, b) synthetic or natural macromolecules or polyelectrolytes, c) viscosity modifiers, d) oil emulsifiers, and e) micro-scale solid supports or coatings.

**Surfactants.** Surfactants are commonly used surface modifiers to control interactions between particles. Several commercially available surfactants were studied for stabilizing nZVI. For instance, Saleh et al. (2007) tested an anionic surfactant, sodium dodecylbenzene-sulfonic acid (SDBS), for post-agglomeration stabilization of a commercial ZVI, and they observed that the sulfonated head groups of SDBS were able to enhance the surface negative potential and thus, the electrostatic repulsion, resulting in smaller ZVI particles and enhanced transportability in porous media. Kanel et al. (2007) prepared nZVI nanoparticles (primary particle size = 2–20 nm) using a nonionic surfactant (Tween 20) as a post-agglomeration stabilizer, and observed improved transport ability and high arsenic removal effectiveness. Basnet et al. (2013) and Bhattacharjee et al. (2016) used a bio-surfactant (Rhamnolipid) and carboxymethyl cellulose (CMC) to stabilize nZVI through the post-agglomeration approach, and they found that Rhamnolipid-stabilized nZVI has a much higher mobility but lower reactivity towards TCE than CMC-stabilized nZVI.

However, when used for *in situ* remediation of soil and groundwater, surfactant stabilizers bear with several critical constraints: 1) effective stabilization can only be achieved at high surfactant concentrations (usually above its critical micelle concentration) (Crane and Scott, 2012), and the surfactant-coated ZVI particles have only limited transportability in real soil; 2) after injection, the surfactant can be rapidly desorbed into groundwater system resulting in weakened stabilization effect (Crane and Scott 2012); 3) the introduced surfactants in the subsurface may solubilize/mobilize non-targeted contaminants; and 4) the surfactants may pose some toxicity concern.

**Synthetic or natural macromolecules or polyelectrolytes.** Compared to surfactants, synthetic polymers and natural biopolymers have been much more widely investigated and

appeared very promising. The macromolecules can not only effectively facilitate pre- or post-agglomeration stabilization of nZVI, but also serve as a food- and energy source for the microbial community. Table 2 summarizes representative stabilizers in this category and key characteristics of the corresponding stabilized nZVI.

**[Table 2]**

Most of the commonly used synthetic polymers (CMC, OMA, PAA, PAP, PMAA-PMMA-PSS, PSS, and PV3A) are negatively charged, while some others (PAM and PVP) are neutral molecules. The negatively charged polymers can be adsorbed on nZVI, resulting in a “quenched” polyelectrolyte layer providing strong electrostatic repulsion (Sirk et al., 2009). Since soil is usually negatively charged, the stabilizer-induced negative potential of nZVI is desired because it diminishes the soil deposition of the nanoparticles when used for in situ remediation (Yan et al., 2013).

Natural biopolymers including guar gum, xanthan gum (XG) and starch are neutral molecules in water. Consequently, steric hindrance and polymer network are the main mechanisms of stabilization. Guar gum and xanthan gum are effective stabilizers for their shear-thinning behavior (Comba et al., 2011). At low shear rate, the gum solution exhibits a high viscosity resulting in stabilization of nZVI. During soil injection, the shear rate will increase and the viscosity of gum-stabilized nZVI suspension can be significantly reduced, which can effectively facilitate the delivery of nZVI (Comba et al., 2011; Vecchia et al., 2009) though much higher injection pressure may be needed compared to anionic stabilizers such as CMC.

Low-cost, food-grade polysaccharides (e.g. starches, celluloses and chitosan) and/or their derivatives can act as effective and “green” stabilizers to yield stable ZVI nanoparticles suitable

for the *in situ* injection uses. These stabilizers are either commercially available or can be easily obtained by modifying natural polysaccharides. These polyhydroxylated and/or polycarboxylated macromolecules possess some novel features, which may prove highly valuable for stabilizing iron-based nanoparticles. First, due to their unique and tunable molecular structure, functionality, and inter- and intra-molecular hydrogen bonding, these macromolecules may serve as effective molecular level capsules that may coat and shield the formed nanoparticles from agglomeration (He and Zhao, 2005, 2007; He et al., 2007; Kim et al., 2003b). Second, they are much cheaper than virtually all other stabilizers tested so far (e.g. cost for a water-soluble starch is \$0.37–\$1.01/kg, and \$5.95/kg for modified carboxymethyl cellulose, or CMC) (He and Zhao, 2005, 2007; He et al., 2010). Third, these natural materials are environmentally friendly and are biocompatible. Fourth, they are mobile in soil and suitable for soil injection uses.

Polysaccharides are considered the most abundant natural biopolymers, and are composed of inter-connected glucose and xylose subunits. More than half polysaccharides are present in the form of starch or cellulose. The primary components of starch are amylose (20–30%) and amylopectin (70–80%). Amylose consists of 100–1000 anhydroglucose units joined by the alpha linkages to form a linear chain structure, whereas amylopectin is much larger, contains branched subunits, and is considered more water-soluble than amylose. Like starch, cellulose also consists of anhydroglucose subunits, which, however, are joined by so-called beta linkages to form a chain structure. Although it is linear and nominally thermoplastic, native cellulose is not readily water-soluble (Shim et al., 2001). However, cellulose can be easily modified to yield derivatives of desired features such as molecular orientation and functionalities (Shim et al., 2001). There are dozens of modified celluloses commercially available, many of which may serve as stabilizers for ZVI nanoparticles. He and Zhao (2005, 2007) and He et al. (2007) developed a

pre-aggregation stabilization technique for preparing highly reactive and soil-deliverable nZVI. They employed a water soluble starch or CMC during particle synthesis, which resulted in much smaller nZVI particles. CMC was found more effective than starch because of the negatively charged carboxymethyl groups ( $pK_a = 4.3$ ), which build a strong surface potential when loaded on the particle surface. For the unprecedented soil deliverability and high reactivity, CMC-stabilized nZVI has been considered most promising for in situ remediation uses, and has been extensively tested in both laboratory and field studies (Bennett et al., 2010; He et al., 2010; Tratnyek et al., 2011). Over the past 10 years or so, the pre-aggregation stabilization strategy using starch or CMC has been also extended to stabilization of many other types of nanoparticles, such as iron sulfide (FeS) (Gong et al., 2012, 2014), magnetite ( $Fe_3O_4$ ) (Liang et al., 2012; Zhang et al., 2010), and vivianite ( $Fe_3(PO_4)_2$ ) (Liu and Zhao, 2007), for various environmental cleanup uses.

Fig. 4 compares the transmission electron microscope (TEM) images of Fe-Pd nanoparticles prepared without a stabilizer (a) and in the presence of starch (b) or CMC (c) (He and Zhao, 2005; 2007). While non-stabilized particles appear as much bulkier (micron-scale) dendritic flocs (Fig. 4a) due to the inter-particle magnetic and van der Waals forces between the particles, starch- or CMC-stabilized nanoparticles appeared as discrete and much finer nanoparticles even after 1 day of aging. The mean particle diameter ( $D$ ) was  $14.1 \pm 11.7$  nm for starched nanoparticles and  $4.3 \pm 1.8$  nm for CMC-stabilized nanoparticles, which translate into a surface area of 55 and  $94 \text{ m}^2 \text{ g}^{-1}$ , respectively. Evidently, the presence of the stabilizers greatly prevented the agglomeration of the resultant iron particles, thereby maintaining the highest surface area of the particles. Further studies revealed that the adsorption of CMC molecules onto the

nanoparticles are due to bidentate bridging between the iron oxide shell of the nanoparticles and the carboxymethyl groups as well as hydrogen bonding (He et al., 2007).

**[Fig. 4]**

The stability or dispersibility of nZVI may be manipulated by varying the concentration of stabilizer and/or using stabilizers of different molecular weights, viscosities, degrees of substitution, or types. For example, the higher the stabilizer concentration, the smaller the particle size, and stabilizers of greater molecular weight give smaller nanoparticles (He and Zhao, 2007).

Saleh et al. (2005) prepared a type of sorptive ZVI particles by coating commercial ZVI particles with synthetic “block copolymer shells” consisting of a hydrophobic inner shell surrounded with a hydrophilic outer shell for dechlorination of dense non-aqueous phase liquids (DNAPLs). Sun et al. (2007) reported that the use of polyvinyl alcohol as a stabilizer can reduce the size of primary ZVI nanoparticles from 60 to 7.9 nm. Based the authors’ estimate, the chemical cost for starch-stabilized nZVI prepared per the pre-agglomeration borohydride reduction approach amounts to \$100/kg and that for CMC-stabilized nZVI to \$120/kg.

**Viscosity modifiers.** Some polymeric molecules can stabilize nZVI by increasing the media viscosity and exerting the polymer network effect. Because solution viscosity is a consequence of the network stiffness, aggregation and sedimentation of nZVI are hindered by the stiffness of the polymer matrix, where the nanoparticles are trapped. Comba and Sethi (2009) reported that both nZVI stability and liquid phase viscosity were enhanced with increasing xanthan gum concentration, and they assumed the stability to be a consequence of the viscosity modification. Xue and Sethi (2012) observed that a viscoelastic gel was formed due to the synergistic

interactions of guar gum and xanthan gum with nZVI, resulting in long-term (>24 h) stabilization of both micro- and nanoscale ZVI particles at concentrations as high as 20 g/L. The stabilization by the gum stabilizers (e.g. xanthan and guar) is attributed to: 1) the greater static viscosity of the mixture, and 2) the yield stress of a polymeric structure that contrasts the downward stress exerted by the iron particles (Xue and Sethi 2012, Xin et al. 2016). Tosco and Sethi (2010) modeled the transport of XG-modified ZVI colloids using a dual-site (physicochemical interactions and straining) advection–dispersion–deposition model and described the shear-thinning behavior that includes a variable apparent viscosity in Darcy’s law. Shear-thinning fluids show decreasing viscosity with increasing shear rate. Consequently, xanthan solutions can enhance stability of the iron dispersion when stored due to the higher static viscosity, yet this process does not hinder the soil injection operations which are conducted at high shear rates (thus lower viscosity). Xin et al. (2016) also claimed that XG is a promising material for field application of nZVI due to its ability to enhance the stability and mobility of nZVI. Sakulchaicharoen et al. (2010) used guar gum as a pre-agglomeration stabilizer during nZVI synthesis, and they found that the viscosity of the guar solution increased from 2.2 cp to 6.0 cp following borohydride addition. The formation of the guar gel and subsequent increases in suspension viscosity hinder the Brownian motion of the nanoparticles, and thus improve the particle stability.

**Oil emulsifiers.** Emulsified nZVI was developed to facilitate delivery of nZVI targeting DNAPL in the subsurface. Food-grade vegetable oils, or oil with commercial surfactants have been used to pack nZVI into oil droplet, i.e., nZVI surrounded by an oil membrane (Berge and Ramsburg, 2009; Quinn et al., 2005). Commercial nZVI was stabilized through post-agglomeration. The hydrophobic oil membrane coating allows DNAPL to concentrate and then

degraded by nZVI inside. The oil membrane also serves as a protective shell to preserve the reactivity of nZVI to avoid corrosion by water and reactions with unwanted groundwater constituents. Using a micro-emulsion method, Li et al. (2003) synthesized nZVI (mean size <10 nm) following a microemulsion method in a water-in-oil microemulsion system made up of n-octane, cetyltrimethyl-ammonium bromide (CTAB), butanol and water, and they observed that the emulsified nZVI offered a 2.6 times faster degradation rate than commercial non-stabilized nZVI.

**Solid supports and protective coatings.** Schrick et al. (2004) employed carbon nanoparticles as supports or “vehicles” for stabilizing and delivering nZVI into porous media. These supports prevent iron particles from agglomeration by shielding the dipolar interactions. In addition, the hydrophobic and inert capping also prolongs the reactivity of the particles and facilitates adsorption of hydrophobic contaminants on the particle surface. Zheng et al. (2008) prepared a class of silica-supported nZVI through an aerosol-assisted process. They claimed that incorporation of nZVI into porous sub-micrometer silica particles protected ferromagnetic iron nanoparticles from aggregation while maintaining the reactivity, and the materials may act as both adsorbents and reducing agents. Column and capillary transport experiments (Zhan et al., 2008) confirmed that the particles move far more effectively through model soils than commercially available nZVI.

Sunkara et al. (2010, 2015) prepared carbon microspheres embedded with nZVI. The Fe/C composite particles are in the optimal size range for transport through soil and the polyelectrolyte (CMC) was able to stabilize the composite microspheres in aqueous solution. Likewise, Mackenzie et al. (2012, 2016) confirmed the effectiveness of Fe/C composites for adsorption and



reduction of halogenated compounds in groundwater. However, CMC or other stabilizers may be needed to further improve stability and the soil deliverability.

In recent years, many more versions of supported nZVI have been reported. While quite promising, many of these supported materials appear more suitable for *ex situ* treatment and/or permeable reactive barriers due to the relatively larger particle size. More details can be found in a recent review by Fu et al. (2014).

### **2.3.3. Comparison of stabilizers.**

Cirtiu et al. (2011) examined four polymeric stabilizers including CMC, PSS, PAA and PAM for stabilizing nZVI synthesized through both pre- and post-agglomeration approaches. For pre-agglomeration stabilization, the mean particle size (measured by TEM) of stabilized nZVI follows the order of: PAA-nZVI (189 nm) > PSS-nZVI (182 nm) > PAM-nZVI (101 nm) > CMC-nZVI (84 nm), indicating that CMC is the most effective stabilizer. When the stabilizers were used for post-agglomeration stabilization, the resulting particle size was comparable in the range of 51.8 to 56.9 nm, indicating that the post-agglomeration may produce smaller nZVI, which is controlled by the efficiency of breaking the ZVI aggregates. However, sedimentation tests demonstrated that the pre-agglomeration stabilized nZVI was more stable, indicating the physically broken particles in the post-agglomeration approach are more prone to re-aggregation. In addition to better colloidal stability, pre-agglomeration stabilization may yield nZVI of higher reactivity (Cho and Choi, 2010; Sakulchaicharoen et al., 2010).

Sakulchaicharoen et al. (2010) examined effectiveness of CMC (M.W.=250kDa), PVP (M.W.=40kDa) and guar gum for nZVI stabilization in the pre-agglomeration stabilization mode. The addition of CMC, PVP and guar gum resulted in nZVI particles with a mean size of 2.8, 74.5

and 63.1 nm, respectively. Sedimentation tests showed that CMC and guar gum can stabilize nZVI for >48 h, compared to <10 h with PVP. In terms of reactivity, the stabilized nZVI showed enhanced reactivity towards TCE, following the order of: CMC-nZVI > PVP-nZVI > guar gum-nZVI > bare ZVI, confirming CMC is the best stabilizer. Lin et al. (2010) compared PAA- and CMC-stabilized nZVI, and found that CMC-stabilized nZVI particles were more amorphous, smaller and more mobile in porous media.

Stabilizers are also compared when used in the post-agglomeration mode. Based on 7-h sedimentation tests, Phenrat et al. (2008a) observed the stabilization effectiveness followed the order of: PSS(70kDa) > PAP(10kDa) > PAP(2.5kDa) > CMC(700kDa) > CMC(90kDa) (numbers in the parentheses indicate M.W.). However, Cirtiu et al. (2011) observed that CMC(90kDa) outperforms PSS(70kDa). The discrepancy can be attributed to many factors that affect post-agglomeration stabilization effectiveness, such as different pH, source ZVI, stabilizer/nZVI ratio and methods used to break up the pre-existing ZVI aggregates. Basnet et al. (2013) and Bhattacharjee et al. (2016) reported that the biosurfactant Rhamnolipid may yield more stable nZVI than CMC with enhanced transportability, but the stabilizer compromised the reactivity towards TCE.

### **3. Applications of stabilized nZVI for environmental remediation**

Stabilized or surface modified ZVI nanoparticles have been widely studied for remediation of both organic and in-organic contaminants in groundwater and soil, as summarized in Fig. 5 and discussed below.

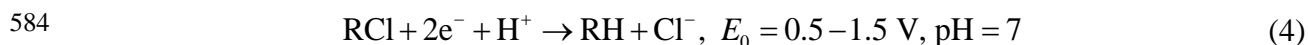
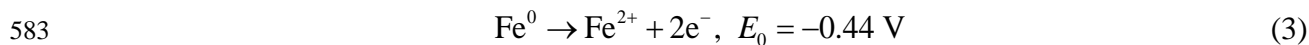
**[Fig. 5]**

Tratnyek et al. (2011) proposed organic coatings may pose four types of effects on the reactivity of ZVI: 1) the organic polyelectrolytes may increase the solubility/mobility of target hydrophobic contaminants, thereby making the contaminants more available for contact with ZVI; 2) organic stabilizers may modify the surface of ZVI, enhancing sorption of contaminants; 3) stabilizers may compete for the reaction sites with target contaminants, thereby inhibiting reactions between ZVI and the contaminants; and 4) stabilizers may serve as a catalyst *via* shuttling electrons, speeding up the redox reactions. More recently, Phenrat et al. (2015) reported that an adsorbed layer of poly(aspartate) on nZVI may “train” and prevent groundwater solutes from blocking nZVI reactive sites. Ou et al. (2016) reported that short-chain organic acids (e.g. oxalic acid) coated on nZVI could enhance dechlorination reactivity due to strong complexation with Fe(II), and thus, decreased formation of ferrous (hydro)oxides, which would precipitate on the nZVI surface and inhibit the reaction.

### **3.1. Applications of stabilized nZVI for transformation of organic contaminants**

The earliest and the most extensive environmental uses of stabilized nZVI have been for reductive degradation of halogenated organics (He and Zhao, 2005). Chlorinated hydrocarbons, such as PCBs, PCE, TCE, DCE, VC and DCA, in soil and groundwater have been a major threat to human and environmental health. ZVI combined with a metal catalyst (mainly Pd) has been shown to be one of the promising materials for reductive degradation of chlorinated solvents due to its moderately strong reducing potential and little known environmental impacts (Urbano and Marinas, 2001).

Eqns. (3) and (4) show the reactions of ZVI corrosion and reduction of aliphatic chlorinated organics by ZVI (Yan et al., 2013):



The key removal processes involve adsorption of chlorinated organics onto the iron surface, and subsequent breakage of the carbon-halogen bonds (Weber, 1996). The reaction can be remarkably speeded up when a small fraction (~0.1wt.% of Fe) of a transition metal, such as Pd, Ni, or Cu, is added. The roles of the metal catalysts include: 1) the galvanic effect and facilitated electron transfer, and 2) enhanced generation of reactive atomic hydrogen (He and Zhao, 2008). Elemental Pd has been found most effective, and thus has been most commonly employed to this end (He and Zhao, 2008). Fig. 6 shows the mechanism for reductive dechlorination by nZVI with or without catalyst Pd. Compared to monometallic nZVI, the Fe-Pd bimetal provides much faster reaction rates, higher removal efficiency and no accumulation of toxic by-products (Lowry and Reinhard, 1999). The key reactions include H<sub>2</sub> production, adsorption of H<sub>2</sub> onto the metal surfaces, formation of reactive hydrogen species, and the subsequent dechlorination reactions. It was reported that Pd buried in the iron oxide shell is less reactive than on the iron surface (Yan et al., 2010c).

#### [Fig. 6]

Dechlorination using granular iron particles is generally very slow. For example, based on the observed pseudo first-order rate constant, the half-life for TCE reduction was found in the order of days or longer (Johnson et al., 1996). As a result, more toxic intermediate by-products such as vinyl chloride may be generated (Xu and Zhang, 2000; Zhang et al., 1998). When applied to PCBs, which are much more persistent, ZVI particles alone are not effective unless under rather extreme conditions (e.g. >300 °C) (Schrack et al., 2002). Because the dechlorination

reaction is a surface-mediated process, increasing the surface area of iron will enhance the reaction kinetics (Arnold and Roberts, 2000). Therefore, reducing the ZVI particle size to the nanoscale using stabilizers can greatly enhance the degradation rate of halogenated organics. For example, He and Zhao (2005) studied the dechlorination of TCE and PCBs using starch-stabilized Fe-Pd nanoparticles, and found that 98% of TCE ( $C_0 = 25$  mg/L) was destroyed within 1 h at a material dose of 0.1 g/L, while 80% of PCBs ( $C_0 = 2.5$  mg/L) was transformed in less than 100 h at a dosage of 1 g/L, as compared to only 24% with non-stabilized Fe-Pd aggregates. They also found that the reactivity (based on the pseudo-first order rate constant) of starch-stabilized Fe-Pd nanoparticles was 37 times faster than that of non-stabilized Fe-Pd nanoparticles with the same Pd loading (0.1 wt.% of ZVI) for TCE degradation and 6 folds faster for PCBs degradation.

CMC-stabilized Fe-Pd nanoparticles showed even greater reactivity than starch-stabilized nZVI. He et al. (2007) found that CMC-stabilized Fe-Pd nanoparticles offered a 2 times faster TCE degradation rate than the starch-stabilized counterparts. The surface-area-based rate constant ( $K_{SA}$ ) was  $0.67 \text{ L h}^{-1} \text{ m}^{-2}$  for the starch-stabilized Fe-Pd nanoparticles (mean size = 14.1 nm) (He and Zhao, 2005), and  $1.56 \text{ L h}^{-1} \text{ m}^{-2}$  for CMC-stabilized Fe-Pd nanoparticles with a mean size of 17.2 nm (He et al., 2007). The primary reason for the enhanced dechlorination reactivity of CMC-stabilized ZVI is the CMC's superior ability to stabilize the nanoparticles and the greater specific reactivity. In addition, the smaller CMC-stabilized nanoparticles may contain more surface reactive atoms (both Fe and Pd) (He et al., 2009a).

Zhang et al. (2011) studied effectiveness of CMC-stabilized Fe-Pd for dechlorination of soil-sorbed TCE. They found that soil adsorption and soil organic matter (SOM) content can limit the dechlorination rate and extent. For instance, ~44% of TCE sorbed on a potting soil ( $\text{TCE} = 0.52$

mg/g, 36 g soil in 63 mL solution, SOM = 8.2%) was degraded by 0.3 g/L CMC-stabilized Fe-Pd nanoparticles in 30 h, compared to ~82% for Smith Farm soil (TCE = 0.45 mg/g, 36 g soil in 63 mL solution, SOM = 0.7%). In addition, the soluble soil organic matter and possibly other soil exudates may inhibit TCE degradation.

In addition to the reductive dechlorination uses, CMC-stabilized Fe-Pd nanoparticles were also capable of facilitating Fenton-like oxidation reactions under aerobic conditions. For example, Joo and Zhao (2008) found that CMC-stabilized nZVI can effectively degrade lindane and atrazine under both aerobic and anaerobic conditions. Under anaerobic conditions, the stabilized nanoparticles serve as a strong electron donor and facilitator of reactive hydrogen species. Under aerobic conditions, the redox reactions between the nanoparticles and DO induce Fenton-like reactions, where reactive radicals are produced, leading to oxidation of the contaminants. However, the researchers observed up to ~50% reduction in •OH production for CMC-stabilized nZVI compared non-stabilized nanoparticles, indicating organic stabilizers may quench reactive species (Joo and Zhao, 2008; Wach et al., 2004).

### **3.2. Applications of stabilized nZVI for removal/immobilization of inorganic contaminants**

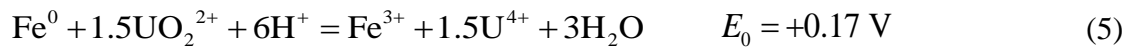
Stabilized ZVI nanoparticles have been investigated for removal or immobilization of numerous inorganic pollutants in soil and water, including heavy metals, metalloids, radionuclides, nitrate, and perchlorate. In general, the remediation approach takes advantage of the high reducing power and much improved soil deliverability. In some cases, ZVI particles, or rather, the iron oxides on the shell, have been used as adsorbents to capture metals or metalloids. However, given the relatively higher cost of nZVI than iron (hydr)oxides particles, it appears less practical to use nZVI only as an adsorbent. For example, it would be more cost-effective to use iron (hydr)oxides than nZVI to adsorb arsenic. However, when reduction reaction is desired,

nZVI would be more advantageous. For instance, nZVI can effectively reduce and immobilize a number of redox-active metals or metalloids such as Cr(VI), U(VI), Tc(VII), Re(VII) and Se(VI) (Liu et al. 2013; Xu and Zhao, 2007). Arsenic contamination has been a world-wide challenge. Arsenic exists in groundwater predominantly as inorganic arsenite ( $\text{H}_3\text{AsO}_3$ ) and arsenate ( $\text{H}_2\text{AsO}_4^-$ , and  $\text{HAsO}_4^{2-}$ ) (Kanel et al., 2005; Smedley and Kinniburgh, 2002). Iron (hydr)oxides on the nZVI shell can serve as a strong adsorbent for both As(V) and As(III) (Kanel et al., 2005). Zhang et al. (2010) compared the effectiveness of starch-stabilized ZVI, FeS and magnetite nanoparticles for immobilization of arsenic in two As-contaminated soils. They found that all the nanoparticles were able to effectively reduce the physiologically based extraction test (PBET) based bioaccessibility and TCLP based leachability of As from the soils. Furthermore, they claimed that nZVI may not be more advantageous over the other cheaper iron-based particles (e.g., magnetite) for arsenic immobilization.

Starch stabilization was found to enhance ZVI's reactivity for the removal of arsenic from aqueous solutions (Mosaferi et al., 2014), which can be attributed to the smaller particle size and greater specific surface area.

Processing of nuclear fuels, radioactive wastes and mining activities have left a legacy of sprawling radionuclides contamination. Treatment of metals and radionuclides in the ground water and vadose zone has been the greatest environmental challenge facing United States Department of Energy (DOE) for decades (Gavrilescu et al., 2009). Among the priority radioactive contaminants are Uranium (U) and Technetium (Tc) due to their high mobility and toxicity (Cui and Eriksen, 1996; Gu et al., 1998). Radionuclides have been detected in groundwater in 70% of US DOE facilities (O'Loughlin et al., 2003). For both U and Tc, the oxidation state is a governing factor for the solubility, mobility and bioavailability (Wersin et al.,

1994). Under reducing conditions, U exists as the insoluble uranium oxide (UO<sub>2</sub>); while under oxidizing conditions, it exists mainly as U(VI), which can hydrolyze and complex with typical ground water ions so as to form soluble and mobile species (Yan et al., 2010a). Consequently, reductive immobilization has been considered a promising technology to mitigate the uranium contamination. Thermodynamically, the reductive immobilization of U(VI) by ZVI can be achieved *via* (Fiedor et al., 1998):



Compared to conventional granular or powder iron materials, nZVI offers much faster kinetics and higher removal efficiency for U(VI). The pseudo-first-order removal rate constant for nZVI at neutral pH was reported to be 678, 1696, and 5 times faster than those by iron flings, galena, and iron sulfide, respectively (Yan et al., 2010a). Noubactep et al. (2003) investigated the effects of various common ions (Cl<sup>-</sup>, CO<sub>3</sub><sup>2-</sup>, NO<sub>2</sub><sup>-</sup>, NO<sub>3</sub><sup>-</sup>, SO<sub>4</sub><sup>2-</sup> and PO<sub>4</sub><sup>3-</sup>), ethylenediamine tetraacetic acid, and humic substances on the U(VI) reduction and co-precipitation by ZVI (scrap iron), and found all the tested ligands inhibited U(VI) removal except for Cl<sup>-</sup>. The inhibitive effect was attributed to surface adsorption and complexation of the ligands at the reactive sites. The researchers also indicated that *in situ* generated corrosion products of ZVI could facilitate irreversible U(VI) uptake. Among these factors, HCO<sub>3</sub><sup>-</sup>, which is ubiquitous in groundwater, can form strong soluble complex with U(VI) in a wide pH range (4–12), thereby severely inhibiting the immobilization effectiveness. For *in situ* immobilization of U(VI) in soil, stabilized nZVI holds great potential.



Like uranium, immobilization of technetium can be achieved by reducing the soluble pertechnetate ( $\text{TcO}_4^-$ ) to the insoluble hydrated oxide form ( $\text{TcO}_2 \cdot n\text{H}_2\text{O}$ ) (Lieser, 1993). Under reducing conditions and at pH 4-10, Tc exists as a precipitate of  $\text{TcO}_2 \cdot n\text{H}_2\text{O}$  and its complexes are also insoluble ( $10^{-7}$  to  $10^{-8}$  mol/L) (Pilkington, 1990). In an acidic solution, the reduction of Tc(VII) to Tc(IV) takes place *via* (Maset et al., 2006):



Liang et al. (1996) studied reductive removal of Tc(VII) by iron filings (size of 420  $\mu\text{m}$ , surface area of  $1.64 \text{ m}^2 \text{ g}^{-1}$ ) at pH 6.2. Under comparable conditions,  $\text{TcO}_4^-$  was rapidly (in 8 h) removed from the aqueous phase by ZVI. The Tc removal was attributed to combination of reductive precipitation and adsorption onto iron filing or oxide surfaces. And the TCLP test showed no significant Tc leaching after the reduction and adsorption. Darab et al. (2007) synthesized zirconia-supported nZVI (size of 10–30, high surface area of  $> 200 \text{ m}^2 \text{ g}^{-1}$ ) and applied to treat a typical Hanford nuclear waste, which contains 0.51 mM  $\text{TcO}_4^-$  at pH 14 and high concentrations of  $\text{Na}^+$ ,  $\text{OH}^-$ ,  $\text{NO}_3^-$  and  $\text{CO}_3^{2-}$ , the nZVI removed 2.4–4.5 times more  $\text{TcO}_4^-$  than commercial iron powder on an equal mass basis. Yet, no studies on removal of Tc using stabilized nZVI have been reported so far.

However, metals or radionuclides immobilized by nZVI may undergo re-oxidation or remobilization depending upon the biogeochemical conditions (especially redox potential) in the subsurface, although information on the long-term stability of in situ stabilized contaminants has been very limited. Flury et al. (2009a, 2009b) reported that ZVI shavings in a field-scale PRB were able to reductively immobilize Cr(VI) via formation of mixed Cr(III)-Fe(III)-hydroxides. However, over four years of monitoring, they observed declined reduction rate, and finally

717 detected Cr(VI) leaching as the ZVI's reduction potential decayed. Tsarev et al. (2016) reported  
718 that while lab-synthesized non-stabilized nZVI was able to immobilize U(VI) in the form of both  
719 nanoparticulate  $\text{UO}_2$  and sorbed U species, and U remained immobilized for up to one year under  
720 anaerobic conditions. However, the immobilized species are susceptible to oxidative dissolution  
721 under aerobic conditions, and they suggested that applications of nZVI to permanently  
722 immobilize U may be limited to sites where strictly anaerobic conditions can be maintained.  
723 Crane et al. (2011) observed non-stabilized nZVI was less effective for treating real U-laden  
724 mine water than for pure U solution, and immobilized U started remobilizing after 1 week and  
725 reached >60% in two weeks in both oxic and anoxic conditions due to interactions with ligands  
726 (especially bicarbonate). Fan et al. (2014) assessed the remobilization of Tc(IV) immobilized by  
727 synthetic nZVI through air-bubbling, and found that 32% of Tc was remobilized during the  
728 initial 20-h oxygenation and 63% within 300 h. The authors asserted that while DO oxidation is  
729 considered the major cause for Tc remobilization, other natural oxidants, such as nitrate and  
730 Mn(IV) oxides may also oxidize Tc(IV). However, information the long-term stability of  
731 immobilized metals or radionuclides using stabilized nZVI has been rare.

732 CMC-stabilized ZVI nanoparticles were found highly effective for reduction of nitrate in  
733 fresh water and brine (Xiong et al., 2009). Batch kinetic tests showed that the pseudo first-order  
734 rate constant for the stabilized nanoparticles was five times greater than that for non-stabilized  
735 counterparts, and the researchers claimed that the stabilizer not only increased the specific  
736 surface area of the nanoparticles, but also increased the particle reactivity. The research also  
737 showed that the final products ( $\text{NH}_4^+$  and  $\text{N}_2$ ) may be manipulated by varying the ZVI-to-nitrate  
738 molar ratio and/or applying an Fe-Cu/Pd bimetallic catalyst, and the greater CMC-to-ZVI ratio  
739 leads to faster nitrate reduction.

Perchlorate is highly water soluble, non-complexing, non-volatile, and chemically stable. It has been highly challenging to remove perchlorate from water by traditional water treatment approaches (Hatzinger, 2005). Xiong et al. (2007) found that ~90% of perchlorate in both fresh water and a simulated ion-exchange brine was destroyed within 7 h by stabilized ZVI at an iron dosage of 1.8 g/L and at moderately elevated temperatures (90–95 °C). An activation energy of 52.59±8.41 kJ/mol was determined for the reaction, which is much lower than non-stabilized ZVI. Perchlorate was rapidly reduced to chloride without accumulation of any intermediate products. The surface-area-normalized rate constant in the presence of starch- or CMC-stabilized ZVI nanoparticles was found to be 1.8 and 3.3 times faster than non-stabilized ZVI for perchlorate degradation, respectively.

### **3.3. Field studies on application of stabilized nZVI for *in situ* remediation**

The first field injection test of nZVI was reported by Elliott and Zhang (2001) for *in situ* degradation of chlorinated organics in groundwater. In this exploratory work, the researchers injected non-stabilized nZVI suspension into the subsurface, and observed that nZVI aggregates rapidly deposited on the well screen while the remaining finer nZVI could travel from a few inches to a few feet before becoming immobilized in the soil matrix. By 2009, the nZVI based *in situ* remediation technology had been demonstrated or tested at the pilot- or field-scale at more than 58 nZVI sites, of which 36 were in the U.S. (Karn et al., 2009). More recently, Bardos et al. (2015) identified around 70 projects documented worldwide at the pilot or full scale. Realizing the very limited soil mobility and deliverability of bare nZVI (Crane and Scott 2012; Grieger et al., 2010), the trend has been moving toward seeking more effective stabilization techniques and more deliverable nZVI.

Quinn et al. (2005) tested the performance of a surfactant-oil emulsified nZVI at a National Aeronautics and Space Administration site to enhance in situ dehalogenation of TCE. The emulsion was injected into eight wells at the depths of 4.9–5.8 m using a pressure pulse injection method. Significant reductions in TCE soil concentrations (>80%) were observed at four of the six soil sampling locations within 90 days of injection, and significant reductions in groundwater TCE concentrations (57-100%) were still observed at all depths targeted with EZVI within 5 months. Further decreases in TCE concentrations were observed in long-term (19 months) groundwater samples, suggesting that a significant portion of the loss of TCE is due to other degradation mechanisms such as biodegradation.

Su et al. (2012) conducted a long-term field test on remediation of chlorinated volatile organic compounds (CVOCs) (primarily PCE) in a subsurface source zone using corn oil and surfactant emulsified nZVI nanoparticles, and they reported 86% reduction in total CVOCs mass and 93% reduction in PCE mass after 2.5 years following the nZVI injection.

He et al. (2010) tested CMC-stabilized Fe-Pd for *in situ* destruction of PCE, TCE and PCBs that had been in a northern Alabama aquifer for decades. Four test wells were installed along the groundwater flow direction (spaced at 1.5 m), including one injection well (IW), one up-gradient monitoring well (MW-3) and two down-gradient monitoring wells (MW-1 and MW-2) (Fig. 7). Stabilized Fe-Pd nanoparticle suspension was prepared on-site right before the injection to preserve the maximum reactivity and then injected into the 50-ft deep, unconfined aquifer. Approximately 568 L (150 gallons) of 0.2 g/L Fe-Pd (CMC = 0.1 wt%, Pd/Fe = 0.1 wt%) was gravity-fed through IW-1 over a 4-h period (Injection #1) and another 150 gallons of 1.0 g/L Fe-Pd (CMC = 0.6 wt%, Pd/Fe = 0.1 wt%) was injected into IW-1 at an injection pressure <5 psi (Injection #2) one month later. Up to ~88% of TCE degradation was observed for over 596 days,

and the study revealed that the nZVI facilitated the rapid abiotic degradation in the initial ~2 weeks. Then, after one month, the delivered stabilized nanoparticles boosted a long-term (nearly two years) biotic dechlorination, where the initial metal corrosion served as an excellent hydrogen source whereas CMC as the carbon source.

**[Fig. 7]**

Bennett et al. (2010) pilot tested the transport and reactivity toward chlorinated ethenes of CMC-stabilized nZVI and Fe-Pd nanoparticles through single well push-pull tests at an existing aerospace facility near San Francisco Bay. They observed that during the push-pull test with stabilized Fe-Pd nanoparticles, ethane concentrations increased from non-detectable to 65 µg/L in extracted groundwater within less than 2 h of reaction time, indicating the rapid abiotic degradation of chlorinated ethenes.

Velimirovic et al. (2014) carried out a pilot injection test with guar gum stabilized microscale (56 µm) ZVI particles at a Belgian site for *in situ* degradation of chlorinated aliphatic hydrocarbons in the subsurface. The suspension was prepared by stabilizing 100 kg ZVI using 1.5 m<sup>3</sup> of guar gum (~ 7 g L<sup>-1</sup>) solution, and was then delivered at 5 depths between 10.5 and 8.5 m through direct push bottom-up injection. Significant abiotic degradation of 1,1,1-TCA was observed near spots where concentrations of ZVI were observed. More recently, Luna et al. (2015) tested by delivering microscale ZVI (guar gum = 2 g/L, ZVI = 10 g/L) into a more permeable soil via controlled-pressure injection (~10 bars), which generated a reactive zone of ~0.8 m around the injection well. One day after injection, the removal of PCE, TCE and cDCE (initial concentrations = 500~3500 µg/L) reached 94%, 96% and 100%, respectively.

### 3.4. Factors affecting properties and effectiveness of stabilized nZVI

Due to the truly nanoscale size and high specific surface area, stabilized ZVI nanoparticles are subject to rapid corrosion and structural/morphological changes, i.e., the physical and chemical properties of nZVI are a strong function of age. nZVI can experience different corrosion mechanisms under anoxic and oxic conditions (Dickinson and Scott, 2010). Compared to non-stabilized ZVI aggregates, stabilized nZVI nanoparticles are subject to faster reactivity loss over time (Wang et al., 2010a). Therefore, stabilized nZVI ought to be used as soon as possible, and storage in aqueous media or exposure to oxygen should be minimized.

Typical ZVI reactions in the aqueous phase are summarized as follows (Dickinson and Scott, 2010):

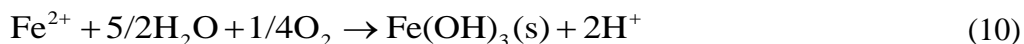
Anoxic corrosion:



Oxic corrosion:



and



Cementation:



where M refers to metals. Based on these reactions, corrosion of the nZVI not only affects the surface and chemical properties of nZVI, but also impacts the aqueous chemistry, such as pH, ionic strength and coexisting ions. As a result, nZVI is typically present as a core-shell structure,

i.e., the ZVI core wrapped in the iron (hydr)oxide (magnetite) shell (Nurmi et al., 2005; Yan et al., 2010b).

The initial nucleation and growth rates during the particle preparation are critical to the stability of the nanoparticles, subsequently affecting the size and stability of the resulting nZVI. As such, some important factors affecting these processes are discussed below.

**Temperature:** The reactivity of nZVI is strongly dependent on synthesis or reaction temperature. According to the Ostwald ripening effect, the higher temperature tends to narrow the size distribution of the nanoparticles due to faster nucleation, competitive growth and the dissolution of smaller particles. In terms of the synthetic reactions (Eqns. 1–2), the higher temperature gives faster redox reaction rate, i.e., formation of more Fe(0) nuclei, which will facilitate faster nucleation and growth of the nanoparticles and is in favor of forming more monodisperse particles (He and Zhao, 2007). In addition, temperature can also affect the solubility, the particle-stabilizer interactions and the effectiveness of stabilizers (Jørgensen et al., 2005).

**Natural organic matter (NOM):** NOM is ubiquitous in the aquatic environment. NOM can affect nZVI functions in the following aspects (Alessi and Li, 2001; Loraine, 2001; Tratnyek et al., 2001): First, NOM can enhance the solubility of hydrophobic organic contaminant, and thus affect the interactions between nZVI and the contaminants. Second, for heavy metals, NOM can form strong complexes, thereby altering the adsorption/immobilization of the metals. Third, NOM adsorbed on nZVI particles can influence the sorption and/or transformation of the contaminants. Fourth, NOM may compete with stabilizers on nZVI surface and affect the size and stability of the particles (typically NOM may lower the stability, giving larger particles). Fifth, the NOM coating on nZVI may form a barrier for electron transfer and mass transfer of the

contaminants, which may prolong the reactive lifetime of nZVI, but also weaken the reactivity toward the contaminants (Zhang et al., 2011).

**pH:** Solution pH plays an important role in nZVI related processes. First, the  $H^+$  activity can influence the reduction of  $Fe^{2+}$  by borohydride during nZVI synthesis, which in turn affects the size and reactivity of the resulting nZVI (Shen et al., 1993). Second, pH can affect the nZVI corrosion, thus affecting the reactive lifetime and reactivity of nZVI for the target contaminants (Eqns. 9–11). Overall, more nZVI will be consumed by reacting with protons at lower pH, which raises solution pH. Moreover, converting  $H^+$  to  $H_2$  by nZVI may result in more reactive atomic hydrogen especially in the presence of a metal catalyst (e.g., Pd or Ni), leading to faster reaction rate (He and Zhao, 2008). In addition, given the core-shell structure of nZVI, pH can affect the surface protonation and charge of nZVI, which will strongly affect uptake of, and reaction with, the ionic contaminants. With respect to the contaminants, pH affects speciation of contaminants, and thus, interactions between the contaminants and nZVI. Lastly, pH may affect speciation of NOM, and thus, NOM-nZVI and NOM-contaminants interactions.

**Ionic strength:** Based on the double-layer theory, the presence of cations can affect the particle stability of nZVI particles. Researchers have reported that the presence of  $Ca^{2+}$  results in larger particle size (more aggregation), and reduces specific surface area and the soil mobility of the particles (He and Zhao 2007). For stabilized nZVI, the presence of the surface coated macromolecules (e.g., CMC) may greatly mitigate the cationic effects because the double layer compression may be less effective when electrosteric interactions are involved. The presence of cations can affect the speciation of contaminants by forming complexes, precipitations or directly competing with target cationic metals.



**Type and concentration of stabilizers.** In general, negatively charged macromolecules (e.g., CMC) are more effective than neutral molecules (e.g., starch), and stabilizers of higher molecular weight are more effective in producing smaller and more reactive nanoparticles (He and Zhao, 2007). However, larger macromolecules are often associated with greater viscosity, which may affect the transport behavior of the nanoparticles. The charge of a stabilizer can greatly alter the surface potential, and thus affect the interactions with the target contaminants. For instance, the zeta potential for CMC-stabilized nZVI can reach -160 mV, while that for starch-stabilized nZVI is nearly zero. Such stabilizer-induced surface potential change can greatly alter the treatment effectiveness. For instance, CMC-stabilized nZVI is less effective toward anionic compounds (e.g., arsenate) than starched counterparts (Liang et al., 2012).

The stabilizer-to-nZVI ratio is an important factor. In general, there exists a minimum stabilizer demand to fully stabilize a given concentration of nanoparticles, which is referred to as the critical stabilization concentration (CSC) (Liang et al, 2012). Higher stabilizer concentrations than CSC may yield even smaller particles and help preserve the reactivity of the nanoparticles. However, too higher concentrations of a stabilizer may also shield some of the reactive sites from interacting with the target contaminants (Liang et al., 2012).

#### **4. Transport of stabilized nZVI**

For practical applications, stabilized nZVI must be mobile enough to be delivered into a target aquifer under some external pressure; yet the delivered nanoparticles should be virtually immobile under typical natural groundwater flow conditions, i.e., once the external injection pressure is released, the nanoparticles should remain within a confined domain; and the stabilizers and the particles must not pose any significant adverse environmental effect.

The classical filtration theory (Kretzschmar et al., 1999) is often invoked to model the transport of stabilized nZVI in porous media. Typically, the retention of nanoparticles in porous media is attributed to three mechanisms: 1) direct interaction of the nanoparticles with the media (interception), 2) sedimentation due to gravity, and 3) diffusion due to Brownian motion (Yao et al., 1971). Under steady saturated flow conditions, the nanoparticle transport can be described by the classic convective-dispersive transport equation with a term accounting for the first-order particle deposition (Kretzschmar et al., 1997). He et al. (2007) demonstrated that ~98% of CMC-stabilized nZVI were detected at full breakthrough through a loamy-sand soil column (1×3.4 cm ID×L), while <0.2% iron was detected for non-stabilized ZVI particles at the column exit. Kanel et al. (2008) reported that PAA-stabilized ZVI could be transported through a 2-dimensional sand box (50×2×28.5 cm L×W×H) without significant retardation. He et al. (2009b) studied the transport of CMC-stabilized iron nanoparticles in four types of porous media (coarse glass bead, fine glass bead, clean sand, and sandy soil) through column tests (1×21 cm ID×L), and the transport data were interpreted using both classical filtration theory and a modified convection-dispersion equation with a first-order removal rate law. They found that a constant concentration plateau was reached at full breakthrough, ranging from 0.99 for glass beads to 0.69 for the soil. The Brownian diffusion was the predominant mechanism for particle breakthrough in all cases, while gravitational sedimentation also played an important role. The attachment efficiency ( $\alpha$ ), representing the fraction of collisions between particles and collectors that result in attachment, for CMC-nZVI was found to be 1–2 orders of magnitude lower than those for ZVI nanoparticles stabilized with other commercial polymers (e.g. PAA and Tween 20). In addition, the particle removal and travel distance are strongly dependent on interstitial flow velocity. The model simulation results indicated that once CMC-stabilized nZVI is delivered, 99% of the

nanoparticles would be removed by the soil matrix within 16 cm at a groundwater flow velocity of 0.1 m/day, but may travel over 146 m at pore flow velocity of 61 m/day, indicating that the transport distance of the nanoparticles can be controlled by manipulating the injection pressure.

Zhang et al. (2016) proposed a mechanistically sounder transport model by incorporating a Langmuir-type adsorption rate law term into the classic convection-dispersion equation with the adsorption parameters derived from independent batch adsorption experiments. The model allows for a quantitative evaluation of the role of adsorption, which is an important mechanism for the retention of stabilized nZVI, especially for soils rich in metals. The model simulation indicated that while filtration is the primary mechanism for particle retention at lower pore flow velocities, adsorption becomes more significant at elevated velocities.

Xu and Zhao (2007) observed high transportability of the CMC-stabilized nZVI nanoparticles (81% of influent CMC-nZVI at full breakthrough) through a sandy loam soil (1×10 cm ID×L), and they claimed that the main reasons for the stabilized nZVI retention in the soil are: 1) some nZVI particles can be intercepted by the soil via the classical filtration mechanisms; and 2) nZVI is gradually oxidized to iron oxides or hydroxides, and eventually completely converted to iron minerals, which are large aggregates and less mobile in soil. Jiemvarangkul et al. (2011) observed that the full breakthrough level for PV3A-stabilized nZVI reached nearly 100%, but only ~43% for PAA-stabilized nZVI, when tested in a sand column (2.5×30 cm ID×L).

The transport behaviors of various stabilized nZVI have been also tested in several field studies. It is now recognized that non-stabilized nZVI is not deliverable to soil/sediment. The field test by Quinn et al. (2005) indicated that the surfactant-oil emulsified ZVI particles were poorly distributed and did not travel as far as expected from each of the injection. In some

locations, the particles migrated up from the injection interval and went off the target. To improve the deliverability, the researchers tested four injection technologies: (a) pneumatic fracturing, (b) hydraulic fracturing, (c) pressure pulsing, and (d) direct injection, and they recommended pneumatic injection and direct push as the most promising technologies to achieve the largest possible radius of influence. However, based on the authors experience, the key technical barrier remains to be controlling the particle aggregation and maximizing the stability. The field test by Su et al. (2012, 2013) showed that the emulsified nZVI was able to travel up to 2.1 m when delivered through pneumatic injection, but only 0.89 m by direct push injection.

The field test by He et al. (2010) demonstrated that when compared with the tracer concentration, approximately 37.4% and 70.0% of the injected CMC-stabilized nZVI was detected in MW-1 during injection #1 and #2, respectively, confirming the soil mobility of the nanoparticles through the aquifer. Furthermore, the authors indicated that the particle transportability can be further improved when the injection pressure or the pore velocity is escalated. Likewise, the push-pull test by Bennett et al. (2010) showed that ~31% of CMC-stabilized nZVI was recovered observed, compared to 76% for the Br<sup>-</sup> tracer, when extraction was performed shortly after the injection; however, only ~2.6% of injected nZVI was recovered, compared to ~61% for the tracer, when extraction was initiated after a 13-h lag time, suggesting that the delivered nZVI particles became essentially immobile over the lag time. The maximum travel distance was estimated to be 1.30 m at the maximum injection pore velocity of 88 m/day. The researchers pointed out that a higher pore velocity during the particle injection increases the advective transport distance of the nanoparticles, and groundwater circulation wells may be employed to facilitate particle delivery and maximize the use of the reactivity of the nanoparticles.

Kocur et al. (2014) field-tested the mobility of CMC-stabilized nZVI at a utility corridor in Sarnia, ON, Canada. They observed that 71% of the injected CMC-nZVI broke through at 1 m from the injection well and remained above 50% for the 24 h injection period, and TEM images showed no discernible morphological changes between the raw and recovered nanoparticles. They suggested that CMC-nZVI could be distributed within at least 1 m radius in the contaminated source zone at sufficient concentrations for degrading the target contaminants (PCE and TCE). The pilot test by Velimirovic et al. (2014) demonstrated that guar gum stabilized microscale ZVI slurries can be directly injected into low permeable aquifers, with a maximum observed delivery distance was 2.5 m; whereas the work by Luna et al. (2015) reported a maximum migration distance of 1.7 m following the direct pressure injection.

## **5. Fate and toxicity of stabilized nZVI**

The stabilized ZVI nanoparticles delivered in the subsurface are expected to be converted to iron minerals in a month or so under the subsurface environmental conditions (Johnson et al., 2013). Under natural groundwater flow conditions, these innocuous minerals are virtually immobile in soil, especially when CMC molecules are degraded by microorganisms, and the particles will eventually be incorporated in the ambient soil matrix. From an environmental remediation aspect, the retained Fe minerals can offer added sorption capacity for a number of toxic chemicals including chromium and arsenic. Through field single well push-pull tests, Bennett et al. (2010) compared the concentrations of a conservative tracer ( $\text{Br}^-$ ) and CMC-stabilized nZVI in extracted groundwater samples, and they indicated that CMC-stabilized nZVI was deliverable in the aquifer but appeared to lose mobility with time, likely due to the interactions (mainly oxidation) between particles and aquifer sediments. Johnson et al. (2013) studied the field-scale transport and transformation of CMC-stabilized nZVI during subsurface

injection in a three-dimensional physical model aquifer (10×10×2.4 m) containing layers of fine, medium and coarse sand. They found that stabilized nZVI was able to transport over up to 2.5 m under very-aggressive flow conditions using a hydraulically constrained flow path between injection and extraction wells. However, total unoxidized nZVI was transported only about 1 m and <2% of the injected nZVI concentration reached that distance. The leading edge of the iron plume became fully oxidized during the transport. However, within the plume, oxidation of nZVI decreased in a fashion consistent with progressive depletion of aquifer “reductant demand”. The time series of water samples from each well exhibits a transition from initially colorless, to yellow and then to black, indicating initial breakthrough of low concentrations of oxidized iron (nZVI<sup>OX</sup>) formed by the reaction of nZVI with oxidizing constituents of the groundwater including water itself, dissolved oxygen, and matrix material, followed by the arrival of black nZVI. The quantity of oxidized iron reflects the “reductant demand” of the aquifer system. The results indicated that rapid oxidation of nZVI not only diminishes the reactivity, but also impedes the soil deliverability.

In the field study done by Su et al. (2012, 2013) at Site 45, they claimed that no nZVI ( $\alpha$ -Fe<sup>0</sup>) was found in most monitoring wells three months after injection, and the injected emulsified nZVI ( $\alpha$ -Fe<sup>0</sup>) was transformed largely to black colored cube-like and plate-like magnetites (Fe<sub>3</sub>O<sub>4</sub>, 0–9 months), then to orange colored irregularly shaped lepidocrocite ( $\gamma$ -FeOOH, 9 months to 2.5 years), then to yellowish lath-like goethite ( $\alpha$ -FeOOH, 2.5 years) and ferrihydrite-like spherical particles in the top portion of the aquifer.

A number of researchers have studied the cytotoxic effects of non-stabilized ZVI. Lee et al. (2008) reported that in pure culture, Lee et al. (2008) found that bare nZVI strongly deactivated *E. coli* under deaerated conditions, with a linear correlation between log inactivation and nZVI

dose and with a log inactivation of 0.82 per mg-Fe/L (compared to <0.017 under air-saturated conditions). The much lower biocidal effects under air-saturation were attributed to the corrosion and surface oxidation of nZVI by DO. The authors proposed the following mechanisms for the strong biocidal effects: 1) physical disruption of the cell membranes, which may cause the inactivation or enhanced the biocidal effects of dissolved iron, 2) reaction of Fe(II) with intracellular oxygen or hydrogen peroxide, which may induce oxidative stress by producing reactive oxygen species, and 3) the reducing power of nZVI may disturb the enzymatic function of external membrane proteins. Moreover, high concentrations of nZVI may induce a strong reducing environment, which can cause an oxidative stress due to the production of reactive oxygen species (e.g.  $\bullet\text{OH}$ ,  $\bullet\text{O}_2^-$  etc.) (El-Temsah and Joner 2013; Joo et al., 2004; Joo et al., 2005; Joo and Zhao 2008).

The toxicological impact of nZVI on indigenous microbial populations (such as soil microorganisms) is more complex. Fajardo et al. (2012) reported that nZVI had little impact on cellular viability and functionality in soil microbiota, while effects on bacteria population are believed to be dose- and species-dependent. A study using marine organisms including mussel, sea squirt and urchin showed that the introduction of nZVI (up to 10 mg/L) can decrease the fertilization success and suppress the embryo developments (Kadar et al., 2013). A phytotoxicity test found strong toxic effect on a plant, *Typh*, when nZVI dose >200 mg/L (Ma et al., 2013). The deposition of iron materials (including nZVI and  $\text{Fe}^{2+}/\text{Fe}^{3+}$  oxides) on the roots could block the membrane pores and substantially reduce the effectiveness of root uptake of water and nutrients, and damage of root and leave cells by the nZVI with strong reducing ability should also not be ignored. However, for aged or exhausted nZVI, toxic influences on earthworms,

collembola and ostracods were observed to be significantly reduced due to decreased reducing power (El-Temsah and Joner, 2012; 2013).

It should be noted that for *in situ* dechlorination, nZVI is often used in the form of bimetallic Fe-Pd nanoparticles, yet information on toxicity of the Fe-Pd nanoparticles has been rare. Murugesan et al. (2011) reported that exposure to nano-scale Fe-Pd (up to 0.1 g/L) had no effect on the growth of *Sphingomonas* sp. PH-07 e and on the cell morphology. There is no information available comparing the toxicity of stabilized bimetallic Fe-Pd and monometallic nZVI. In the contrary, field tests (He and Zhao, 2010) reported that the organic coating (e.g., CMC, used as pre-agglomeration stabilizer) of nZVI can serve as a potential carbon source and iron corrosion as the H<sub>2</sub> source for anaerobic bacteria, and thus boost the biological activity in soil. Kocur et al., 2015 observed similar stimulated biotic degradation of chlorinated compounds following injection of CMC stabilized nZVI, and in addition, they found increased local populations of organohalide-respiring microorganisms. Lab tests also revealed that CMC stabilized nZVI had less adverse effect on *Agrobacterium* sp. compared to bare nZVI. Apparently, the negative CMC coating prevents interactions between the nanoparticles and bacteria and suppresses the available reactive oxygen species (ROS).

The toxicity is highly dosage-dependent (Kim et al., 2010; Xiu et al., 2010), and was found to be diminished in the presence of NOM, polyelectrolytes (CMC or OMA) or an aquifer matrix, indicating the toxic effects in real-world systems are likely much lower than under the lab-simulated conditions (Li et al., 2010). Researchers reported that anionic coatings such as CMC can greatly alleviate the toxic effects, for instance, 5 mg/L of non-stabilized nZVI has the equivalent toxic effect to 500 mg/L of CMC-stabilized nZVI towards *E. coli*. (Lee et al., 2008; Li et al., 2010). Phenrat et al. (2008b) also reported the PAA-modified nZVI showed lower



neurotoxicity to cultured rodent microglia (BV2) and neurons (N27) than nZVI and “aged” nZVI (>11 months). It was interesting that although the PAA-nZVI had substantially more Fe<sup>0</sup> content than the “aged” nZVI, surface coating resulted in reduced ROS production, suggesting an independent effect of the PAA coating rather than the “redox” activity of the materials. Studies also demonstrated that low doses of nZVI may not affect the bacteria population and growth, though the population structure and composition may be altered (Kim et al., 2010; Xiu et al., 2010). Recently, a more thorough comparison between bare and CMC stabilized nZVI (post-agglomeration) was conducted by Dong et al. (2016). The survival tests of *E. coli* demonstrated that the addition of 0.01 wt% of CMC only slightly decrease the toxicity of nZVI, while greater reduction and almost complete reduction of cytotoxicity of nZVI was observed at CMC dose of 0.03 and 1.6 wt%. The TEM image clearly showed that the CMC stabilized nZVI did not appear to destroy membrane integrity of *E. coli* due to the CMC coating. In addition, after the CMC stabilized nZVI aged for 15 or 30 days, the resulted iron oxides exhibits almost no toxicity.

According to Eqns (1) and (2), the nZVI suspension prepared by the borohydride reduction method contains significant amounts of borates (mainly, boric acid and tetrahydroxyborate). Kozma et al. (2015) claimed that the resulting oxidized boron species during nZVI synthesis cannot be easily separated from the nZVI product and they are strictly prohibited from entering groundwater bodies in several countries. Liu et al. (2005) reported that the resulting monometallic Fe(B) particles contain 86 wt% Fe<sup>0</sup> and 5 wt% boron, and appear largely amorphous. While detailed information on the environmental fate and toxicity of nZVI-associated borates is lacking, existing toxicological data on borates suggest that borates introduced through nZVI injection may not constitute a serious threat. Based on a rat developmental toxicity study with a NOAEL of 9.6 mg B/kg/day for borax and boric, Murray

(1995) obtained a human Reference Dose of 0.3 mg B/kg/day and an acceptable daily intake of 18 mg B/day, which translated into a safe level of 8.25 mg B/L in drinking water.

## **6. *In situ* remediation using stabilized nZVI: merits and limitations**

Stabilized ZVI nanoparticles offer the unique advantage of being soil deliverable and highly reactive toward many important contaminants in soil and groundwater, which warrants the development of a new *in situ* remediation technology by directly delivering the nanoparticles into the contaminated source zone. Fig. 8 presents a schematic diagram summarizing the preparation and applicaiton of stabilized nZVI for *in situ* remediation of contaminated soil and groundwater. The life cycle of stabilized nZVI can be summarized as: a) Preparation of stabilized nZVI by pre- or post-agglomeration stabilization methods; b) Delivery of stabilized nZVI into the soil for *in situ* remediation of typical contaminants (both organics and inorganics); c) Effectively utilize the reducing power of the delivered nanoparticles to degrade the target contaminants; and d) Transformation of nZVI in the subsurface into iron oxides or hydroxides, desorption, and decomposition of the stabilizers.

### **[Fig. 8]**

Compared to traditional remediation practices such as PRBs, pump-and-treat, and excavating and landfill, the *in situ* technology holds the potential to be not only much less environmentally destructive, but also cost-effective, i.e., it may greatly cut down the remediation timeframe and cost (EPA, 2004; Karn et al., 2009; Piquepaille, 2003). In addition, the technology can reach contaminants that are not reachable with conventional technologies, such as contaminants located in deep acquirers or those underneath surface barriers (He et al., 2010), where the *in situ* technology may be the only possible solution.

The most promising uses of stabilized nZVI are for reductive degradation of redox-active organics (e.g., halogenated compounds) and reductive immobilization of redox-active metals, metalloids, and radionuclides (e.g., Cr(VI), U(VI) and Tc(VII)). Given that such redox-active contaminants are widespread, the *in situ* remediation technology based on stabilized nZVI holds the potential to greatly innovate the current remediation practices. Although the particle stabilization has greatly improved the particle deliverability, the transport and soil delivery remains the bottle neck for the technology, especially when used for less permeable soil or sediment. Moreover, as sorption/desorption and diffusion of contaminants often limit the physical and biological availabilities of contaminants, and as the reactive lifetime of stabilized nZVI is fairly short, the technology may not be suitable for sites where contaminant desorption is slow. Some leachable soil components may inhibit the reactivity of nZVI, and high concentrations of DOM and cations may affect particle size and reactivity (Zhang et al., 2011). Particle oxidation should be avoided. nZVI can be oxidized due to reactions with water, DO and soil/groundwater components (e.g., metals and MnO<sub>2</sub>).

Information on the fate of nZVI delivered in the field soil remains limited. The geochemical and biochemical conditions in groundwater and subsurface can significantly alter the properties of nZVI. Conversely, the application of nZVI to the subsurface may alter the local biogeochemical conditions (e.g., dissolution of iron oxide minerals) which in turn may affect contaminant stability.

## **7. Technical constraints and future research needs**

Like any other new technologies, the nZVI-based *in situ* technology bears with some critical constraints and this review reveals the following knowledge gaps and further research needs:

- a) Although the particle stabilization technique (especially the use of CMC) has greatly improved the soil deliverability of nZVI, the transport distance remains a bottle neck for effective application of the technology, especially for soil of low permeability. There is a need to further modify the particle stabilization technique to yield more soil dispersible nanoparticles and to facilitate the deliverability of stabilized nZVI to contaminated source zones.
- b) It has been challenging to extend the reactive lifetime of nZVI. It is likely to use a combination of stabilizers of various properties (e.g., M.W. or hydrophobicity) to minimize the corrosion reactions with water while maintaining high reactivity toward the target contaminants.
- c) Information on the long-term stability of metals/radionuclides immobilized by stabilized nZVI is missing. Such long-term monitoring data, especially in the field-scale, are critical to assess the technology effectiveness and optimize the process design.
- d) While no evidence has shown that stabilized nZVI can pose significant toxic effects on biota under environmentally relevant conditions and dosages, our knowledge on the long-term environmental impacts remains rudimentary. More research is needed to understand the effects of delivered nZVI on the local biological systems. Moreover, there is a need to investigate the bio-toxicity of stabilized bimetallic (e.g., Fe-Pd) nanoparticles.
- e) Further studies are needed to investigate how delivered nZVI affects the biogeochemical conditions and mobility of other chemicals in the subsurface, in particular under the field settings; likewise, the effects of local environmental conditions on the fate, transport and transformation of nZVI should be investigated.

- f) The effect of the delivered nanoparticles on the hydraulic conductivity should be further confirmed at the field scale and over extended period of time.
- g) Mechanistically sounder transport model that considers chemical transformation of nZVI is needed for better predicting the transport and fate of stabilized nZVI in soil.
- h) There is a need to further study the synergistic or antagonistic effects of nZVI and microbial activities.

## 8. Conclusions

The particle stabilization technique using low-cost and “green” polysaccharides provided a valuable alternative for preparing soil-deliverable nZVI and represents a great step toward field application of the in situ remediation technology. Depending on site characteristics and properties of the target contaminants, neutral or charged polysaccharides may be used to yield stabilized nZVI of desired particle size and transportability. The pre-agglomeration stabilization technique is not only thermodynamically more favorable, but also more effective in fabricating smaller nanoparticles and facilitating size control. In addition to much improved soil deliverability, stabilized nZVI shows greater reactivity and much lower adverse cytotoxicity. The effectiveness and feasibility of stabilized nZVI for remediation of both organic and inorganic contaminants have been widely tested or demonstrated in the laboratory, pilot and field scales, which revealed great potential and technical constraints as well. Overall, the use of stabilized nZVI appears more suitable where the strong reduction is desired, e.g., reductive dehalogenation and reductive immobilization of metals or radionuclides; whereas it appears less cost-effective when nZVI is used merely as an adsorbent. The status quo warrants further the need for development focusing on field demo-testing and interactions between stabilized nZVI and local biogeochemical conditions.

## Acknowledgments

This work was partially supported by the National Natural Science Foundation of China (Grant 41230638), the Higher Education Doctoral Program Foundation from the Ministry of Education of China, and a grant from the USDA AAES 2015 Hatch and Multistate funding program.

## References

- Agrawal, A., Tratnyek, P.G., 1995. Reduction of nitro aromatic compounds by zero-valent iron metal. *Environmental Science & Technology* 30(1), 153-160.
- Alessi, D.S., Li, Z.H., 2001. Synergistic effect of cationic surfactants on perchloroethylene degradation by zero-valent iron. *Environmental Science & Technology* 35(18), 3713-3717.
- Arnold, W.A., Roberts, A.L., 2000. Pathways and kinetics of chlorinated ethylene and chlorinated acetylene reaction with Fe(0) particles. *Environmental Science & Technology* 34(9), 1794-1805.
- Bardos P., Bone B., Daly P., Elliott D., Jones S., Lowry G.V., Merly C., 2015. A risk/benefit appraisal for the application of nano-scale zero valent iron (nZVI) for the remediation of contaminated sites. Report for European Union Seventh Framework Programme.
- Basnet, M., Ghoshal, S., Tufenkji, N., 2013. Rhamnolipid biosurfactant and soy protein act as effective stabilizers in the aggregation and transport of palladium-doped zerovalent iron nanoparticles in saturated porous media. *Environmental Science & Technology* 47(23), 13355-13364.
- Bennett, P., He, F., Zhao, D., Aiken, B., Feldman, L., 2010. *In situ* testing of metallic iron nanoparticle mobility and reactivity in a shallow granular aquifer. *Journal of Contaminant Hydrology* 116(1-4), 35-46.
- Berge, N.D., Ramsburg, C.A., 2009. Oil-in-water emulsions for encapsulated delivery of reactive iron particles. *Environmental Science & Technology* 43(13), 5060-5066.
- Bhattacharjee, S., Basnet, M., Tufenkji, N., Ghoshal, S., 2016. Effects of rhamnolipid and carboxymethylcellulose coatings on reactivity of palladium-doped nanoscale zerovalent iron particles. *Environmental Science & Technology* 50(4), 1812-1820.
- Brown, H.C., Brown, C.A., 1962. A simple preparation of highly active platinum metal catalysts for catalytic hydrogenation. *Journal of the American Chemical Society* 84(8), 1494-1495.
- Chatterjee, J., Haik, Y., Chen, C.J., 2002. Polyethylene magnetic nanoparticle: a new magnetic material for biomedical applications. *Journal of Magnetism and Magnetic Materials* 246(3), 382-391.
- Cho, Y., Choi, S.I., 2010. Degradation of PCE, TCE and 1, 1, 1-TCA by nanosized FePd bimetallic particles under various experimental conditions. *Chemosphere* 81(7), 940-945.
- Cirtiu, C.M., Raychoudhury, T., Ghoshal, S., Moores, A., 2011. Systematic comparison of the size, surface characteristics and colloidal stability of zero valent iron nanoparticles pre-and post-grafted with common polymers. *Colloids and Surfaces A: Physicochemical and Engineering Aspects* 390(1), 95-104.

1199 Comba, S., Dalmazzo, D., Santagata, E., Sethi, R., 2011. Rheological characterization of xanthan suspensions  
1200 of nanoscale iron for injection in porous media. *Journal of Hazardous Materials* 185(2), 598-605.

1201 Comba, S., Sethi, R., 2009. Stabilization of highly concentrated suspensions of iron nanoparticles using shear-  
1202 thinning gels of xanthan gum. *Water Research* 43(15), 3717-3726.

1203 Corrias, A., Ennas, G., Licheri, G., Marongiu, G., Paschina, G., 1990. Amorphous metallic powders prepared  
1204 by chemical-reduction of metal-ions with potassium borohydride in aqueous-solution. *Chemistry of*  
1205 *Materials* 2(4), 363-366.

1206 Crane, R.A., Dickinsona, M., Popescub, I.C. Scotta, T.B. 2011. Magnetite and zero-valent iron nanoparticles  
1207 for the remediation of uranium contaminated environmental water. *Water Research* 45(9), 2931–2942.

1208 Crane, R.A., Scott, T., 2012. Nanoscale zero-valent iron: Future prospects for an emerging water treatment  
1209 technology. *Journal of Hazardous Materials* 211, 112-125.

1210 Cui, D.Q., Eriksen, T.E., 1996. Reduction of pertechnetate by ferrous iron in solution: Influence of sorbed and  
1211 precipitated Fe(II). *Environmental Science & Technology* 30(7), 2259-2262.

1212 Darab, J.G., Amonette, A.B., Burke, D.S.D., Orr, R.D., Ponder, S.M., Schrick, B., Mallouk, T.E., Lukens,  
1213 W.W., Caulder, D.L., Shuh, D.K., 2007. Removal of pertechnetate from simulated nuclear waste streams  
1214 using supported zerovalent iron. *Chemistry of Materials* 19(23), 5703-5713.

1215 Dickinson, M., Scott, T.B., 2010. The application of zero-valent iron nanoparticles for the remediation of a  
1216 uranium-contaminated waste effluent. *Journal of Hazardous Materials* 178(1-3), 171-179.

1217 Dong, H., Xie, Y., Zeng, G., Tang, L., Liang, J., He, Q., Zhao, F., Zeng Y., Wu, Y., 2016. The dual effects of  
1218 carboxymethyl cellulose on the colloidal stability and toxicity of nanoscale zero-valent iron.  
1219 *Chemosphere*, 144, 1682-1689.

1220 Elliott, D.W., Zhang, W.X., 2001. Field assessment of nanoscale bimetallic particles for groundwater treatment.  
1221 *Environmental Science & Technology* 35(24), 4922-4926.

1222 El-Temsah, Y.S., Joner, E.J., 2012. Ecotoxicological effects on earthworms of fresh and aged nano-sized zero-  
1223 valent iron (nZVI) in soil. *Chemosphere* 89(1), 76-82.

1224 El-Temsah, Y.S., Joner, E.J., 2013. Effects of nano-sized zero-valent iron (nZVI) on DDT degradation in soil  
1225 and its toxicity to collembola and ostracods. *Chemosphere* 92(1), 131-137.

1226 EPA, 2004. Federal Remediation Technologies Roundtable Meeting, Arlington, VA, June 9, 2004.  
1227 <http://www.frtr.gov/pdf/meetings/frtr1298.pdf>.

1228 Fajardo, C., Ortíz, L.T., Rodríguez-Membibre, M.L., Nande, M., Lobo, M.C., Martin, M., 2012. Assessing the  
1229 impact of zero-valent iron (ZVI) nanotechnology on soil microbial structure and functionality: A  
1230 molecular approach. *Chemosphere* 86(8), 802-808.

1231 Fan, D., Anitori, R. P., Tebo, B. M., Tratnyek, P. G., Lezama Pacheco, J. S., Kukkadapu, R. K., Bowden, M.  
1232 E., 2014. Oxidative remobilization of technetium sequestered by sulfide-transformed nano zerovalent iron.  
1233 *Environmental science & technology* 48(13), 7409-7417.

1234 Fiedor, J.N., Bostick, W.D., Jarabek, R.J., Farrell, J., 1998. Understanding the mechanism of uranium removal  
1235 from groundwater by zero-valent iron using X-ray photoelectron spectroscopy. *Environmental Science &*  
1236 *Technology* 32(10), 1466-1473.

1237 Fu, F., Dionysiou, D.D., Liu, H., 2014. The use of zero-valent iron for groundwater remediation and  
1238 wastewater treatment: A review. *Journal of Hazardous Materials* 267, 194-205.

1239 Flury, B., Eggenberger, U., Mäder, U., 2009a. First results of operating and monitoring an innovative design of  
 1240 a permeable reactive barrier for the remediation of chromate contaminated groundwater. *Applied*  
 1241 *Geochemistry* 24(4), 687-696.

1242 Flury, B., Frommer, J., Eggenberger, U., Mäder, U., Nachttegaal, M., Kretzschmar, R., 2009b. Assessment of  
 1243 long-term performance and chromate reduction mechanisms in a field scale permeable reactive barrier.  
 1244 *Environmental Science & Technology* 43(17), 6786-6792.

1245 Gavrilescu, M., Pavel, L.V., Cretescu, I., 2009. Characterization and remediation of soils contaminated with  
 1246 uranium. *Journal of Hazardous Materials* 163(2), 475-510.

1247 Gillham R.W., 1993. Cleaning halogenated contaminants from groundwater: U.S. Patent No. 5, 266, 213. 1993;  
 1248 11-30.

1249 Gillham, R.W., 2003. Discussion of papers/discussion of nano-scale iron for dehalogenation. *Groundwater*  
 1250 *Monitoring & Remediation* 23(1), 6-8.

1251 Gillham, R.W., Ohannesin, S.F., 1994. Enhanced degradation of halogenated aliphatics by zero-valent iron.  
 1252 *Ground Water* 32(6), 958-967.

1253 Glavee, G.N., Klabunde, K.J., Sorensen, C.M., Hadjipanayis, G.C., 1995. Chemistry of borohydride reduction  
 1254 of iron(II) and iron(III) ions in aqueous and nonaqueous media-formation of nanoscale Fe, Fe<sub>2</sub>O<sub>3</sub>, and Fe<sub>3</sub>O<sub>4</sub>  
 1255 powders. *Inorganic Chemistry* 34(1), 28-35.

1256 Gong, Y., Liu, Y., Xiong, Z., Kaback, D., Zhao, D., 2012. Immobilization of mercury in field soil and  
 1257 sediment using carboxymethyl cellulose stabilized iron sulfide nanoparticles. *Nanotechnology* 23(29),  
 1258 294007.

1259 Gong, Y., Liu, Y., Xiong, Z., Zhao, D., 2014. Immobilization of mercury by carboxymethyl cellulose  
 1260 stabilized iron sulfide nanoparticles: reaction mechanisms and effects of stabilizer and water chemistry.  
 1261 *Environmental Science & Technology* 48(7), 3986-3994.

1262 Gould, J., 1982. The kinetics of hexavalent chromium reduction by metallic iron. *Water Research* 16(6), 871-  
 1263 877.

1264 Grieger, K.D., Fjordbøge, A., Hartmann, N.B., Eriksson, E., Bjerg, P.L., Baun, A., 2010. Environmental  
 1265 benefits and risks of zero-valent iron nanoparticles (nZVI) for *in situ* remediation: Risk mitigation or  
 1266 trade-off? *Journal of Contaminant Hydrology* 118(3), 165-183.

1267 Gu, B., Liang, L., Dickey, M.J., Yin, X., Dai, S., 1998. Reductive precipitation of uranium(VI) by zero-valent  
 1268 iron. *Environmental Science & Technology* 32(21), 3366-3373.

1269 Guan, X., Sun, Y., Qin, H., Li, J., Lo, I.M., He, D., Dong, H., 2015. The limitations of applying zero-valent  
 1270 iron technology in contaminants sequestration and the corresponding countermeasures: The development  
 1271 in zero-valent iron technology in the last two decades (1994–2014). *Water Research* 75, 224-248.

1272 Hatzinger, P.B., 2005. Perchlorate biodegradation for water treatment. *Environmental Science & Technology*  
 1273 39(11), 239A-247A.

1274 He, F., Liu, J., Roberts, C.B., Zhao, D., 2009a. One-step “green” synthesis of Pd nanoparticles of controlled  
 1275 size and their catalytic activity for trichloroethene hydrodechlorination. *Industrial & Engineering*  
 1276 *Chemistry Research* 48(14), 6550-6557.

1277 He, F., Zhang, M., Qian, T., Zhao, D., 2009b. Transport of carboxymethyl cellulose stabilized iron  
 1278 nanoparticles in porous media: Column experiments and modeling. *Journal of Colloid and Interface*  
 1279 *Science* 334(1), 96-102.



1280 He, F., Zhao, D., 2005. Preparation and characterization of a new class of starch-stabilized bimetallic  
 1281 nanoparticles for degradation of chlorinated hydrocarbons in water. *Environmental Science &*  
 1282 *Technology* 39(9), 3314-3320.

1283 He, F., Zhao, D., 2007. Manipulating the size and dispersibility of zerovalent iron nanoparticles by use of  
 1284 carboxymethyl cellulose stabilizers. *Environmental Science & Technology* 41(17), 6216-6221.

1285 He, F., Zhao, D., 2008. Hydrodechlorination of trichloroethene using stabilized Fe-Pd nanoparticles: Reaction  
 1286 mechanism and effects of stabilizers, catalysts and reaction conditions. *Applied Catalysis B:*  
 1287 *Environmental* 84(3), 533-540.

1288 He, F., Zhao, D., Liu, J., Roberts, C.B., 2007. Stabilization of Fe-Pd nanoparticles with sodium carboxymethyl  
 1289 cellulose for enhanced transport and dechlorination of trichloroethylene in soil and groundwater.  
 1290 *Industrial & Engineering Chemistry Research* 46(1), 29-34.

1291 He, F., Zhao, D., Paul, C., 2010. Field assessment of carboxymethyl cellulose stabilized iron nanoparticles for  
 1292 *in situ* destruction of chlorinated solvents in source zones. *Water Research* 44(7), 2360-2370.

1293 Hoag, G.E., Collins, J.B., Holcomb, J.L., Hoag, J.R., Nadagouda, M.N., Varma, R.S., 2009. Degradation of  
 1294 bromothymol blue by 'greener' nano-scale zero-valent iron synthesized using tea polyphenols. *Journal of*  
 1295 *Materials Chemistry* 19(45), 8671-8677.

1296 Huber, D.L., 2005. Synthesis, properties, and applications of iron nanoparticles. *Small* 1(5), 482-501.

1297 Hydutsky, B.W., Mack, E.J., Beckerman, B.B., Skluzacek, J.M., Mallouk, T.E., 2007. Optimization of nano-  
 1298 and microiron transport through sand columns using polyelectrolyte mixtures. *Environmental science &*  
 1299 *technology* 41(18), 6418-6424.

1300 Jiemvarangkul, P., Zhang, W.X., Lien, H.L., 2011. Enhanced transport of polyelectrolyte stabilized nanoscale  
 1301 zero-valent iron (nZVI) in porous media. *Chemical Engineering Journal* 170(2-3), 482-491.

1302 Johnson, R.L., Nurmi, J.T., Johnson, G.S.O.B., Fan, D., Johnson, R.L.O.B., Shi, Z., Salter-Blanc, A.J.,  
 1303 Tratnyek, P.G., Lowry, G.V., 2013. Field-scale transport and transformation of carboxymethylcellulose-  
 1304 stabilized nano zero-valent iron. *Environmental Science & Technology* 47(3), 1573-1580.

1305 Johnson T.L., Scherer M.M., Tratnyek P.G., 1996. Kinetics of halogenated organic compound degradation by  
 1306 iron metal. *Environmental Science & Technology* 30(8), 2634-2640.

1307 Joo, S. H., Feitz, A. J., Sedlak, D. L., Waite, T. D., 2005. Quantification of the oxidizing capacity of  
 1308 nanoparticulate zero-valent iron. *Environmental science & technology* 39(5), 1263-1268.

1309 Joo, S. H., Feitz, A. J., Waite, T. D., 2004. Oxidative degradation of the carbothioate herbicide, molinate, using  
 1310 nanoscale zero-valent iron. *Environmental science & technology* 38(7), 2242-2247.

1311 Joo, S.H., Zhao, D., 2008. Destruction of lindane and atrazine using stabilized iron nanoparticles under aerobic  
 1312 and anaerobic conditions: Effects of catalyst and stabilizer. *Chemosphere* 70(3), 418-425.

1313 Jørgensen, J.M., Erlacher, K., Pedersen, J.S., Gothelf, K.V., 2005. Preparation temperature dependence of size  
 1314 and polydispersity of alkylthiol monolayer protected gold clusters. *Langmuir* 21(23), 10320-10323.

1315 Kadar, E., Dyson, O., Handy, R.D., Al-Subiai, S.N., 2013. Are reproduction impairments of free spawning  
 1316 marine invertebrates exposed to zero-valent nano-iron associated with dissolution of nanoparticles?  
 1317 *Nanotoxicology* 7(2), 135-143.

1318 Kanel, S.R., Goswami, R.R., Clement, T.P., Barnett, M.O., Zhao, D., 2008. Two dimensional transport  
1319 characteristics of surface stabilized zero-valent iron nanoparticles in porous media. *Environmental*  
1320 *Science & Technology* 42(3), 896-900.

1321 Kanel, S.R., Manning, B., Charlet, L., Choi, H., 2005. Removal of arsenic(III) from groundwater by nanoscale  
1322 zero-valent iron. *Environmental Science & Technology* 39(5), 1291-1298.

1323 Kanel, S.R., Nepal, D., Manning, B., Choi, H., 2007. Transport of surface-modified iron nanoparticle in porous  
1324 media and application to arsenic(III) remediation. *Journal of Nanoparticle Research* 9(5), 725-735.

1325 Karn, B., Kuiken, T., Otto, M., 2009. Nanotechnology and *in situ* remediation: a review of the benefits and  
1326 potential risks. *Environmental Health Perspectives* 117(12), 1823-1831.

1327 Kim, D.K., Mikhaylova, M., Wang, F.H., Kehr, J., Bjelke, B., Zhang, Y., Tsakalakos, T., Muhammed, M.,  
1328 2003a. Starch-coated superparamagnetic nanoparticles as MR contrast agents. *Chemistry of Materials*  
1329 15(23), 4343-4351.

1330 Kim, D.K., Mikhaylova, M., Zhang, Y., Muhammed, M., 2003b. Protective coating of superparamagnetic iron  
1331 oxide nanoparticles. *Chemistry of Materials* 15(8), 1617-1627.

1332 Kim, J.Y., Park, H.J., Lee, C., Nelson, K.L., Sedlak, D.L., Yoon, J., 2010. Inactivation of *Escherichia coli* by  
1333 nanoparticulate zerovalent iron and ferrous ion. *Applied and Environmental Microbiology* 76(22), 7668-  
1334 7670.

1335 Kocur, C.M., Chowdhury, A.I., Sakulchaicharoen, N., Boparai, H.K., Weber, K.P., Sharma, P., Krol, M.M.,  
1336 Austrins, L., Peace, C., Sleep, B.E., O'Carroll, D.M., 2014. Characterization of nZVI mobility in a field  
1337 scale test. *Environmental Science & Technology* 48(5), 2862-2869.

1338 Kocur, C.M., Lomheim, L., Boparai, H.K., Chowdhury, A.I., Weber, K.P., Austrins, L.M., Edwards, E.A.,  
1339 Sleep, B.E., O'Carroll, D.M., 2015. Contributions of abiotic and biotic dechlorination following  
1340 carboxymethyl cellulose stabilized nanoscale zero valent iron injection. *Environmental Science &*  
1341 *Technology* 49(14), 8648-8656.

1342 Kozma, G., Rónavári, A., Kónya, Z., Kukovecz, A., 2015. Environmentally benign synthesis methods of zero-  
1343 valent iron nanoparticles. *ACS Sustainable Chemistry & Engineering* 4(1), 291-297.

1344 Kretzschmar, R., Barmettler, K., Grolimund, D., Yan, Y.D., Borkovec, M., Sticher, H., 1997. Experimental  
1345 determination of colloid deposition rates and collision efficiencies in natural porous media. *Water*  
1346 *Resources Research* 33(5), 1129-1137.

1347 Kretzschmar, R., Borkovec, M., Grolimund, D., Elimelech, M., 1999. *Advances in Agronomy*. Donald, L.S.  
1348 (ed), pp. 121-193, Academic Press.

1349 Laurent, S., Forge, D., Port, M., Roch, A., Robic, C., Vander Elst, L., Muller, R.N., 2008. Magnetic iron oxide  
1350 nanoparticles: synthesis, stabilization, vectorization, physicochemical characterizations, and biological  
1351 applications. *Chemical Reviews* 108(6), 2064-2110.

1352 Lee, C., Kim, J.Y., Lee, W.I., Nelson, K.L., Yoon, J., Sedlak, D.L., 2008. Bactericidal effect of zero-valent  
1353 iron nanoparticles on *Escherichia coli*. *Environmental Science & Technology* 42(13), 4927-4933.

1354 Li, F., Vipulanandan, C., Mohanty, K.K., 2003. Microemulsion and solution approaches to nanoparticle iron  
1355 production for degradation of trichloroethylene. *Colloids and Surfaces A-Physicochemical and*  
1356 *Engineering Aspects* 223(1-3), 103-112.

1357 Li, S., Yan, W., Zhang, W.X., 2009. Solvent-free production of nanoscale zero-valent iron (nZVI) with  
1358 precision milling. *Green Chemistry* 11(10), 1618-1626.

1359 Li, Z., Greden, K., Alvarez, P.J., Gregory, K.B., Lowry, G.V., 2010. Adsorbed polymer and NOM limits  
1360 adhesion and toxicity of nano scale zerovalent iron to *E. coli*. *Environmental Science & Technology* 44(9),  
1361 3462-3467.

1362 Liang, L.Y., Gu, B.H., Yin, X.P., 1996. Removal of technetium-99 from contaminated groundwater with  
1363 sorbents and reductive materials. *Separations Technology* 6(2), 111-122.

1364 Liang, Q., Zhao, D., Qian, T., Freeland, K., Feng, Y., 2012. Effects of stabilizers and water chemistry on  
1365 arsenate sorption by polysaccharide-stabilized magnetite nanoparticles. *Industrial & Engineering*  
1366 *Chemistry Research* 51(5), 2407-2418.

1367 Lieser, K.H., 1993. Technetium in the nuclear-fuel cycle, in medicine and in the environment. *Radiochimica*  
1368 *Acta* 63, 5-8.

1369 Lin, C.L., Lee, C.F., Chiu, W.Y., 2005. Preparation and properties of poly (acrylic acid) oligomer stabilized  
1370 superparamagnetic ferrofluid. *Journal of Colloid and Interface Science* 291(2), 411-420.

1371 Lin, Y.H., Tseng, H.H., Wey, M.Y., Lin, M.D., 2010. Characteristics of two types of stabilized nano zero-  
1372 valent iron and transport in porous media. *Science of the Total Environment* 408(10), 2260-2267.

1373 Liu, H., Qian, T., Zhao, D., 2013. Reductive immobilization of perhenate in soil and groundwater using  
1374 starch-stabilized ZVI nanoparticles. *Chinese Science Bulletin* 58(2), 275-281.

1375 Liu, R., Zhao, D., 2007. Reducing leachability and bioaccessibility of lead in soils using a new class of  
1376 stabilized iron phosphate nanoparticles. *Water Research* 41(12), 2491-2502.

1377 Liu, W., Tian, S., Zhao, X., Xie, W., Gong, Y., Zhao, D., 2015. Application of stabilized nanoparticles for *in*  
1378 *situ* remediation of metal-contaminated soil and groundwater: A critical review. *Current Pollution Reports*  
1379 1(4), 280-291.

1380 Liu, Y.F., Choi, H., Dionysiou, D, Lowry, G.V., 2005. Trichloroethene hydrodechlorination in water by highly  
1381 disordered monometallic nanoiron. *Chemistry of Materials*. 17, 5315-5322.

1382 Loraine, G.A., 2001. Effects of alcohols, anionic and nonionic surfactants on the reduction of PCE and TCE by  
1383 zero-valent iron. *Water Research* 35(6), 1453-1460.

1384 Louie, S.M., Tilton, R.D., Lowry, G.V., 2016. Critical review: Impacts of macromolecular coatings on critical  
1385 physicochemical processes controlling environmental fate of nanomaterials. *Environmental Science:*  
1386 *Nano* 3, 283-310.

1387 Lowry, G.V., Reinhard, M., 1999. Hydrodehalogenation of 1- to 3-carbon halogenated organic compounds in  
1388 water using a palladium catalyst and hydrogen gas. *Environmental Science & Technology* 33(11), 1905-  
1389 1910.

1390 Luna, M., Gastone F., Tosco T., Sethi R., Velimirovic M., Gemoets J., Muyschond R., Sapion H., Klaas N.,  
1391 Bastiaens L., 2015. Pressure-controlled injection of guar gum stabilized microscale zerovalent iron for  
1392 groundwater remediation. *Journal of Contaminant Hydrology* 181, 46-58. Ma, X., Gurung, A., Deng, Y.,  
1393 2013. Phytotoxicity and uptake of nanoscale zero-valent iron (nZVI) by two plant species. *Science of the*  
1394 *Total Environment*, 443, 844-849.

1395 Mackenzie, K., Bleyl, S., Georgi, A., Kopinke, F.D., 2012. Carbo-Iron—an Fe/AC composite—as alternative to  
1396 nano-iron for groundwater treatment. *Water Research* 46(12), 3817-3826.

1397 Mackenzie, K., Bleyl, S., Kopinke, F.D., Doose, H., Bruns, J., 2016. Carbo-Iron as improvement of the  
1398 nanoiron technology: From laboratory design to the field test. *Science of the Total Environment*. (In  
1399 Press).

1400 Maset, E.R., Sidhu, S.H., Fisher, A., Heydon, A., Worsfold, P.J., Cartwright, A.J., Keith-Roach, M.J., 2006.  
 1401 Effect of organic co-contaminants on technetium and rhenium speciation and solubility under reducing  
 1402 conditions. *Environmental Science & Technology* 40(17), 5472-5477.

1403 Matheson, L.J., Tratnyek, P.G., 1994. Reductive dehalogenation of chlorinated methanes by iron metal.  
 1404 *Environmental Science & Technology* 28(12), 2045-2053.

1405 Mondal, K., Jegadeesan, G., Lalvani, S.B., 2004. Removal of selenate by Fe and NiFe nanosized particles.  
 1406 *Industrial & Engineering Chemistry Research* 43(16), 4922-4934.

1407 Mosaferi, M., Nemati, S., Khataee, A., Nasser, S., Hashemi, A.A., 2014. Removal of Arsenic (III, V) from  
 1408 aqueous solution by nanoscale zero-valent iron stabilized with starch and carboxymethyl cellulose.  
 1409 *Journal of Environmental Health Science and Engineering* 12(1), 74.

1410 Murray, F.J., 1995. A human health risk assessment of boron (boric acid and borax) in drinking  
 1411 water. *Regulatory Toxicology and Pharmacology* 22(3), 221-230.

1412 Murugesan, K., Bokare, V., Jeon, J.R., Kim, E. J., Kim, J.H., Chang, Y.S., 2011. Effect of Fe-Pd bimetallic  
 1413 nanoparticles on *Sphingomonas* sp. PH-07 and a nano-bio hybrid process for triclosan  
 1414 degradation. *Bioresource technology* 102(10), 6019-6025.

1415 Mykhaylyk, O., Cherchenko, A., Ilkin, A., Dudchenko, N., Ruditsa, V., Novoseletz, M., Zozulya, Y., 2001.  
 1416 Glial brain tumor targeting of magnetite nanoparticles in rats. *Journal of Magnetism and Magnetic*  
 1417 *Materials* 225(1), 241-247.

1418 Njagi, E.C., Huang, H., Stafford, L., Genuino, H., Galindo, H.M., Collins, J.B., Hoag, G.E., Suib, S.L., 2010.  
 1419 Biosynthesis of iron and silver nanoparticles at room temperature using aqueous sorghum bran extracts.  
 1420 *Langmuir* 27(1), 264-271.

1421 Noubactep, C., Meinrath, G., Dietrich, P., Merkel, B., 2003. Mitigating uranium in groundwater: Prospects and  
 1422 limitations. *Environmental Science & Technology* 37(18), 4304-4308.

1423 Nurmi, J.T., Tratnyek, P.G., Sarathy, V., Baer, D.R., Amonette, J.E., Pecher, K., Wang, C., Linehan, J.C.,  
 1424 Matson, D.W., Penn, R.L., 2005. Characterization and properties of metallic iron nanoparticles:  
 1425 spectroscopy, electrochemistry, and kinetics. *Environmental Science & Technology* 39(5), 1221-1230.

1426 O'Loughlin, E.J., Kelly, S.D., Cook, R.E., Csencsits, R., Kemner, K.M., 2003. Reduction of uranium(VI) by  
 1427 mixed iron(II)/iron(III) hydroxide (green rust): Formation of UO<sub>2</sub> nanoparticles. *Environmental Science*  
 1428 *& Technology* 37(4), 721-727.

1429 O'Hannesin, S.F., Gillham, R.W., 1992. A permeable reaction wall for *in situ* degradation of halogenated  
 1430 organic compounds. The 45<sup>th</sup> Canadian Geotechnical Society Conference, 25-28 October 1992, Toronto,  
 1431 Ontario, Canada.

1432 Ou, Y. H., Wei, C. Y., Shih, Y. H., 2016. Short-chain organic acids increase the reactivity of zerovalent iron  
 1433 nanoparticles toward polychlorinated aromatic pollutants. *Chemical Engineering Journal* 284, 372-379.

1434 Pardoe, H., Chua-Anusorn, W., Pierre, T.G.S., Dobson, J., 2001. Structural and magnetic properties of  
 1435 nanoscale iron oxide particles synthesized in the presence of dextran or polyvinyl alcohol. *Journal of*  
 1436 *Magnetism and Magnetic Materials* 225(1), 41-46.

1437 Phenrat, T., Cihan, A., Kim, H.J., Mital, M., Illangasekare, T., Lowry, G.V., 2010. Transport and deposition of  
 1438 polymer-modified Fe<sup>0</sup> nanoparticles in 2-D heterogeneous porous media: Effects of particle concentration,  
 1439 Fe<sup>0</sup> content, and coatings. *Environmental Science & Technology* 44(23), 9086-9093.

1440 Phenrat, T., Liu, Y., Tilton, R.D., Lowry, G.V., 2009. Adsorbed polyelectrolyte coatings decrease Fe<sup>0</sup>  
 1441 nanoparticle reactivity with TCE in water: conceptual model and mechanisms. *Environmental Science &*  
 1442 *Technology* 43(5), 1507-1514.

1443 Phenrat, T., Long, T.C., Lowry, G.V., Veronesi, B., 2008b. Partial oxidation (“aging”) and surface  
 1444 modification decrease the toxicity of nanosized zerovalent iron. *Environmental Science & Technology*  
 1445 43(1), 195-200.

1446 Phenrat, T., Saleh, N., Sirk, K., Kim, H.J., Tilton, R.D., Lowry, G.V., 2008a. Stabilization of aqueous  
 1447 nanoscale zerovalent iron dispersions by anionic polyelectrolytes: adsorbed anionic polyelectrolyte layer  
 1448 properties and their effect on aggregation and sedimentation. *Journal of Nanoparticle Research* 10(5),  
 1449 795-814.

1450 Phenrat, T., Schoenfelder, D., Kirschling, T. L., Tilton, R. D., Lowry, G. V., 2015. Adsorbed poly (aspartate)  
 1451 coating limits the adverse effects of dissolved groundwater solutes on Fe<sup>0</sup> nanoparticle reactivity with  
 1452 trichloroethylene. *Environmental Science and Pollution Research*, 1-13.

1453 Pilkington, N.J., 1990. The solubility of technetium in the near-field environment of a radioactive-waste  
 1454 repository. *Journal of the Less-Common Metals* 161(2), 203-212.

1455 Piquepaille, R. 2003, Cleaning the Environment with Iron Nanoparticles. Roland Piquepaille's Technology  
 1456 Trends, <http://radio.weblogs.com/0105910/2003/09/05.html#a577>.

1457 Quinn, J., Geiger, C., Clausen, C., Brooks, K., Coon, C., O'Hara, S., Krug, T., Major, D., Yoon, W.S.,  
 1458 Gavaskar, A., Holdsworth, T., 2005. Field demonstration of DNAPL dehalogenation using emulsified  
 1459 zero-valent iron. *Environmental Science & Technology* 39(5), 1309-1318.

1460 Sakulchaicharoen, N., O'Carroll, D.M., Herrera, J.E., 2010. Enhanced stability and dechlorination activity of  
 1461 pre-synthesis stabilized nanoscale FePd particles. *Journal of Contaminant Hydrology* 118(3), 117-127.

1462 Saleh, N., Phenrat, T., Sirk, K., Dufour, B., Ok, J., Sarbu, T., Matyjaszewski, K., Tilton, R.D., Lowry,  
 1463 G.V., 2005. Adsorbed triblock copolymers deliver reactive iron nanoparticles to the oil/water interface.  
 1464 *Nano Letter* 5(12), 2489-2494.

1465 Saleh, N., Sirk, K., Liu, Y., Phenrat, T., Dufour, B., Matyjaszewski, K., Tilton, R.D., Lowry, G. V., 2007.  
 1466 Surface modifications enhance nanoiron transport and NAPL targeting in saturated porous media.  
 1467 *Environmental Engineering Science* 24(1), 45-57.

1468 Schlesinger, H.I., Brown, H.C., Finholt, A.E., Gilbreath, J.R., Hoekstra, H.R., Hyde, E.K., 1953. New  
 1469 developments in the chemistry of diborane and of the borohydrides .9. Sodium borohydride, its hydrolysis  
 1470 and its use as a reducing agent and in the generation of hydrogen. *Journal of the American Chemical*  
 1471 *Society* 75(1), 215-219.

1472 Schrick, B., Blough, J.L., Jones, A.D., Mallouk, T.E., 2002. Hydrodechlorination of trichloroethylene to  
 1473 hydrocarbons using bimetallic nickel-iron nanoparticles. *Chemistry of Materials* 14(12), 5140-5147.

1474 Schrick, B., Hydutsky, B.W., Blough, J.L., Mallouk, T.E., 2004. Delivery vehicles for zerovalent metal  
 1475 nanoparticles in soil and groundwater. *Chemistry of Materials* 16(11), 2187-2193.

1476 Senzaki, T., 1991. Removal of chlorinated organic compounds from wastewater by reduction process: III.  
 1477 Treatment of trichloroethylene with iron powder. *Kogyo Yosui* 391, 29-35.

1478 Senzaki, T., Kumagai, Y., 1988a. Removal of chlorinated organic compounds from wastewater by reduction  
 1479 process: Treatment of 1, 1, 2, 2-tetrachloroethane with iron powder. *Kogyo Yosui* 357(2), 2-7.

1480 Senzaki, T., Kumangai, Y., 1988b. Removal of chlorinated organic compounds from wastewater by reduction  
1481 process: II. Treatment of tetrachloroethane with iron powder. *Kogyo Yosui* 369, 19-25.

1482 Shen, J., Li, Z., Yan, Q., Chen, Y., 1993. Reactions of bivalent metal ions with borohydride in aqueous  
1483 solution for the preparation of ultrafine amorphous alloy particles. *The Journal of Physical Chemistry*  
1484 97(32), 8504-8511.

1485 Shim, I.W., Choi, S., Noh, W.T., Kwon, J., Cho, J.Y., Chae, D.Y., Kim, K.S., 2001. Preparation of iron  
1486 nanoparticles in cellulose acetate polymer and their reaction chemistry in the polymer. *Bulletin-Korean*  
1487 *Chemical Society* 22(7), 772-774.

1488 Sirk, K.M., Saleh, N.B., Phenrat, T., Kim, H.J., Dufour, B., Ok, J., Golas, P.L., Matyjaszewski, K., Lowry,  
1489 G.V., Tilton, R.D., 2009. Effect of adsorbed polyelectrolytes on nanoscale zero valent iron particle  
1490 attachment to soil surface models. *Environmental Science & Technology* 43(10), 3803-3808.

1491 Smedley, P.L., Kinniburgh, D.G., 2002. A review of the source, behaviour and distribution of arsenic in  
1492 natural waters. *Applied Geochemistry* 17(5), 517-568.

1493 Su, C., Puls, R.W., Krug, T.A., Watling, M.T., O'Hara, S.K., Quinn, J.W., Ruiz, N.E., 2012. A two and half-  
1494 year-performance evaluation of a field test on treatment of source zone tetrachloroethene and its  
1495 chlorinated daughter products using emulsified zero valent iron nanoparticles. *Water Research* 46(16),  
1496 5071-5084.

1497 Su, C., Puls, R. W., Krug, T. A., Watling, M. T., O'Hara, S. K., Quinn, J. W., Ruiz, N. E., 2013. Travel  
1498 distance and transformation of injected emulsified zerovalent iron nanoparticles in the subsurface during  
1499 two and half years, *Water Research*, 47(12), 4095-4106.

1500 Sun, S., Zeng, H., 2002. Size-controlled synthesis of magnetite nanoparticles. *Journal of the American*  
1501 *Chemical Society* 124(28), 8204-8205.

1502 Sun, Y.P., Li, X.Q., Zhang, W.X., Wang, H.P., 2007. A method for the preparation of stable dispersion of  
1503 zero-valent iron nanoparticles. *Colloids and Surfaces A-Physicochemical and Engineering Aspects* 308(1-  
1504 3), 60-66.

1505 Sunkara, B., Su, Y., Zhan, J., He, J., McPherson, G.L., John, V.T., 2015. Iron-carbon composite microspheres  
1506 prepared through a facile aerosol-based process for the simultaneous adsorption and reduction of  
1507 chlorinated hydrocarbons. *Frontiers of Environmental Science & Engineering* 9(5), 939-947.

1508 Sunkara, B., Zhan, J., He, J., McPherson, G.L., Piringer, G., John, V.T., 2010. Nanoscale zerovalent iron  
1509 supported on uniform carbon microspheres for the *in situ* remediation of chlorinated hydrocarbons. *ACS*  
1510 *Applied Materials & Interfaces* 2(10), 2854-2862.

1511 Suslick, K.S., Fang, M., Hyeon, T., 1996. Sonochemical synthesis of iron colloids. *Journal of the American*  
1512 *Chemical Society* 118(47), 11960-11961.

1513 Tiraferri, A., Chen, K.L., Sethi, R., Elimelech, M., 2008. Reduced aggregation and sedimentation of zero-  
1514 valent iron nanoparticles in the presence of guar gum. *Journal of Colloid and Interface Science* 324(1),  
1515 71-79.

1516 Tiraferri, A., Sethi, R., 2009. Enhanced transport of zerovalent iron nanoparticles in saturated porous media by  
1517 guar gum. *Journal of Nanoparticle Research* 11(3), 635-645.

1518 Tosco, T., Papini, M.P., Viggi, C.C., Sethi, R., 2014. Nanoscale zerovalent iron particles for groundwater  
1519 remediation: A review. *Journal of Cleaner Production* 77, 10-21.

1520 Tosco, T., Sethi, R., 2010. Transport of non-Newtonian suspensions of highly concentrated micro-and  
 1521 nanoscale iron particles in porous media: a modeling approach. *Environmental Science &*  
 1522 *Technology* 44(23), 9062-9068.

1523 Tratnyek, P.G., Johnson, R.L., 2006. Nanotechnologies for environmental cleanup. *Nano today* 1(2), 44-48.

1524 Tratnyek, P.G., Salter-Blanc, A., Nurmi, J., Amonette, J.E., Liu, J., Wang, C.M., Dohnalkova, A., Baer, D.R.,  
 1525 2011. Reactivity of zerovalent metals in aquatic media: Effects of organic surface coatings, ACS  
 1526 Symposium Series. American Chemical Society 1071, 381-406.

1527 Tratnyek, P.G., Scherer, M.M., Deng, B.L., Hu, S.D., 2001. Effects of natural organic matter, anthropogenic  
 1528 surfactants, and model quinones on the reduction of contaminants by zero-valent iron. *Water Research*  
 1529 35(18), 4435-4443.

1530 Tsarev, S., Collins, R.N., Fahy, A., Waite, T.D., 2016. Reduced uranium phases produced from anaerobic  
 1531 reaction with nanoscale zerovalent iron. *Environmental Science & Technology* 50(5), 2595-2601.

1532 Urbano, F.J., Marinas, J.M., 2001. Hydrogenolysis of organohalogen compounds over palladium supported  
 1533 catalysts. *Journal of Molecular Catalysis A-Chemical* 173(1-2), 329-345.

1534 van Wonerghem, J., Mørup, S., Charles, S.W., Wells, S., Villadsen, J., 1985. Formation of a metallic glass by  
 1535 thermal decomposition of  $\text{Fe}(\text{CO})_5$ . *Physical Review Letters* 55(4), 410.

1536 van Wonerghem, J., Mørup, S., Koch, C.J., Charles, S.W., Wells, S., 1986. Formation of ultra-fine amorphous  
 1537 alloy particles by reduction in aqueous solution. *Nature* 322, 622-623.

1538 Vecchia, E.D., Luna, M., Sethi, R., 2009. Transport in porous media of highly concentrated iron micro-and  
 1539 nanoparticles in the presence of xanthan gum. *Environmental Science & Technology* 43(23), 8942-8947.

1540 Velimirovic, M. Tosco, T., Uytteboek, M., Luna, M., Gastone, F., De Boer, C., Klaas, N., Spaion, H.,  
 1541 Eisenmann, H., Lasson, P.O., Braun, J., Sethi, R., Bastiaens, L., 2014. Field assessment of guar gum  
 1542 stabilized microscale zerovalent iron particles for *in-situ* remediation of 1,1,1-trichloroethane. *Journal of*  
 1543 *Contaminated Hydrology* 164, 88-99.

1544 Wach, R.A., Kudoh, H., Zhai, M., Nagasawa, N., Muroya, Y., Yoshii, F., Katsumura, Y., 2004. Rate constants  
 1545 of reactions of carboxymethylcellulose with hydrated electron, hydroxyl radical and the decay of CMC  
 1546 macroradicals. A pulse radiolysis study. *Polymer* 45(24), 8165-8171.

1547 Wang, C.B., Zhang, W.X., 1997. Synthesizing nanoscale iron particles for rapid and complete dechlorination  
 1548 of TCE and PCBs. *Environmental Science & Technology* 31(7), 2154-2156.

1549 Wang, Q., Lee, S., Choi, H., 2010a. Aging study on the structure of  $\text{Fe}^0$ -nanoparticles: stabilization,  
 1550 characterization, and reactivity. *Journal of Physical Chemistry C* 114(5), 2027-2033.

1551 Wang, Q., Qian, H., Yang, Y., Zhang, Z., Naman, C., Xu, X., 2010b. Reduction of hexavalent chromium by  
 1552 carboxymethyl cellulose-stabilized zero-valent iron nanoparticles. *Journal of Contaminant Hydrology*  
 1553 114(1-4), 35-42.

1554 Weber, E.J., 1996. Iron-mediated reductive transformations: investigation of reaction mechanism.  
 1555 *Environmental Science & Technology* 30(2), 716-719.

1556 Wersin, P., Hochella, M.F., Persson, P., Redden, G., Leckie, J.O., Harris, D.W., 1994. Interaction between  
 1557 aqueous uranium(VI) and sulfide minerals: Spectroscopic evidence for sorption and reduction.  
 1558 *Geochimica et Cosmochimica Acta* 58(13), 2829-2843.

1559 Xin, J., Tang, F., Zheng, X., Shao, H., Kolditz, O., 2016. Transport and retention of xanthan gum-stabilized  
1560 microscale zero-valent iron particles in saturated porous media. *Water Research* 88, 199-206.

1561 Xiong, Z., Zhao, D., Pan, G., 2007. Rapid and complete destruction of perchlorate in water and ion-exchange  
1562 brine using stabilized zero-valent iron nanoparticles. *Water Research* 41(15), 3497-3505.

1563 Xiong, Z., Zhao, D., Pan, G., 2009. Rapid and controlled transformation of nitrate in water and brine by  
1564 stabilized iron nanoparticles. *Journal of Nanoparticle Research* 11(4), 807-819.

1565 Xiu, Z.M., Gregory, K.B., Lowry, G.V., Alvarez, P.J.J., 2010. Effect of bare and coated nanoscale zerovalent  
1566 iron on *tceA* and *vcrA* gene expression in *Dehalococcoides* spp. *Environmental Science & Technology*  
1567 44(19), 7647-7651.

1568 Xu, J., Bhattacharyya, D., 2005. Membrane-based bimetallic nanoparticles for environmental remediation:  
1569 Synthesis and reactive properties. *Environmental Progress* 24(4), 358-366.

1570 Xu, Y., Zhang, W.X., 2000. Subcolloidal Fe/Ag particles for reductive dehalogenation of chlorinated benzenes.  
1571 *Industrial & Engineering Chemistry Research* 39(7), 2238-2244.

1572 Xu, Y., Zhao, D., 2007. Reductive immobilization of chromate in water and soil using stabilized iron  
1573 nanoparticles. *Water Research* 41(10), 2101-2108.

1574 Xue, D., Sethi, R., 2012. Viscoelastic gels of guar and xanthan gum mixtures provide long-term stabilization  
1575 of iron micro-and nanoparticles. *Journal of Nanoparticle Research*, 14(11), 1-14.

1576 Yan, W., Herzing, A.A., Li, X.Q., Kiely, C.J., Zhang, W.X., 2010a. Structural evolution of Pd-doped  
1577 nanoscale zero-valent iron (nZVI) in aqueous media and implications for particle aging and reactivity.  
1578 *Environmental Science & Technology* 44(11), 4288-4294.

1579 Yan, S., Hua, B., Bao, Z.Y., Yang, J., Liu, C.X., Deng, B.L., 2010b. Uranium(VI) removal by nanoscale  
1580 zerovalent iron in anoxic batch systems. *Environmental Science & Technology* 44(20), 7783-7789.

1581 Yan, W., Herzing, A.A., Kiely, C.J., Zhang, W.X., 2010c. Nanoscale zero-valent iron (nZVI): aspects of the  
1582 core-shell structure and reactions with inorganic species in water. *Journal of Contaminant Hydrology*  
1583 118(3), 96-104.

1584 Yan, W., Lien, H.L., Koel, B.E., Zhang, W.X., 2013. Iron nanoparticles for environmental clean-up: Recent  
1585 developments and future outlook. *Environmental Science: Processes & Impacts* 15(1), 63-77.

1586 Yao, K.M., Habibian, M.T., O'Melia, C.R., 1971. Water and waste water filtration. Concepts and applications.  
1587 *Environmental Science & Technology* 5(11), 1105-1112.

1588 Zhan, J.J., Zheng, T.H., Piringer, G., Day, C., McPherson, G.L., Lu, Y.F., Papadopoulos, K., John, V.T., 2008.  
1589 Transport characteristics of nanoscale functional zerovalent iron/silica composites for *in situ* remediation  
1590 of trichloroethylene. *Environmental Science & Technology* 42 (23), 8871-8876.

1591 Zhang, M., He, F., Zhao, D., Hao, X., 2011. Degradation of soil-sorbed trichloroethylene by stabilized zero  
1592 valent iron nanoparticles: Effects of sorption, surfactants, and natural organic matter. *Water Research*  
1593 45(7), 2401-2414.

1594 Zhang, M., He, F., Zhao, D., Hao, X., 2016. Transport of stabilized iron nanoparticles in porous media: Effects  
1595 of surface and solution chemistry and role of adsorption. *Journal of Hazardous Materials*. (In Press)

1596 Zhang, M., Wang, Y., Zhao, D., Pan, G., 2010. Immobilization of arsenic in soils by stabilized nanoscale zero-  
1597 valent iron, iron sulfide (FeS), and magnetite (Fe<sub>3</sub>O<sub>4</sub>) particles. *Chinese Science Bulletin* 55(4-5), 365-  
1598 372.



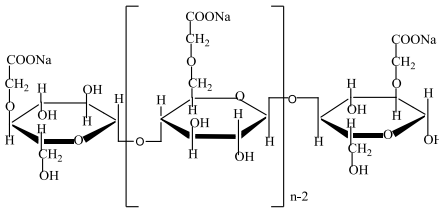
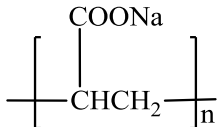
- 1599 Zhang, W.X., 2003. Nanoscale iron particles for environmental remediation: an overview. Journal of  
1600 Nanoparticle Research 5(3-4), 323-332.
- 1601 Zhang, W.X., Wang, C.B., Lien, H.L., 1998. Treatment of chlorinated organic contaminants with nanoscale  
1602 bimetallic particles. Catalysis Today 40(4), 387-395.
- 1603 Zheng, T.H., Zhan, J.J., He, J.B., Day, C., Lu, Y.F., McPherson, G.L., Piringer G., John, V.T., 2008. Reactivity  
1604 characteristics of nanoscale zerovalent iron-silica composites for trichloroethylene remediation. Environmental  
1605 Science & Technology 42 (12), 4494-4499.

## Tables

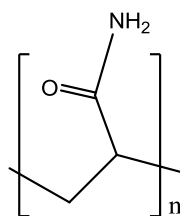
**Table 1.** A summary of some important review papers on nZVI.

Publication date	Focus area	Reference
2003	The earliest summary of synthesis, characterization, reactivity and <i>in situ</i> field tests for non-stabilized nZVI	(Zhang, 2003)
2006	Morphology, reactivity and mobility of nZVI. Comparison of <i>in situ</i> and <i>ex situ</i> application of nZVI	(Tratnyek and Johnson, 2006)
2006	Materials and engineering aspects of non-stabilized nZVI	(Li et al., 2006)
2010	Effects of organic coating on reactivity of ZVI or nZVI	(Tratnyek et al., 2011)
2012	Perspectives on nZVI injection strategy	(Crane and Scott, 2012)
2013	Updated account of developments and field experiences of nZVI	(Yan et al., 2013)
2014	Use of ZVI or nZVI for groundwater remediation and wastewater treatment	(Fu et al., 2014)
2014	Use of nZVI for groundwater remediation	(Tosco et al., 2014)
2015	Limitations and recent developments of ZVI and nZVI	(Guan et al., 2015)
2015	Use of stabilized nanomaterials for metal contaminants in soil/groundwater	(Liu et al., 2015)
2016	Interactions between macromolecular coatings and nanomaterials	(Louie et al., 2016)

**Table 2.** Summary and comparison of synthetic polymers and natural biopolymers as nZVI stabilizers and key characteristics.

Code	Key properties of stabilizer	Structure of stabilizer	Remarks	Reference
<b>Synthetic polymers/polyelectrolytes</b>				
CMC	Carboxymethyl cellulose. Food grade polysaccharide. Nontoxic and biodegradable. Weak anionic functional groups (pKa=4.3). M.W. = 90K. CMC binds with nZVI through bidentate bridging.		<p><b>Pre-agglomeration:</b> nZVI:stabilizer mass ratio* = 1:20. Very effective, can attain discrete stable nZVI (Mean size = 4.3 nm).</p> <p><b>Post-agglomeration:</b> nZVI:stabilizer = 1:0.33. Effective for commercial RNIP. Less effective than pre-agglomeration method. Particles may flocculate. Coating thickness = ~7 nm.</p>	He and Zhao 2007
OMA	Olefin maleic acid. Weak anionic polyelectrolyte. M.W. = 16K. Used as NOM analog due to similar functional groups and properties in natural waters.	N/A	<p><b>Post-agglomeration:</b> nZVI:stabilizer = 1:3.2. Mean hydrodynamic diameter by dynamic light scattering (DLS) = 253 nm. Transportable through sands. More effective than PSS (see below).</p>	Phenrat et al., 2010
PAA	Polyacrylate acid. Weak anionic polyelectrolyte. M.W.=1.8K. Binds with ZVI through chelation of polyacid to the iron (hydr)oxide shell.		<p><b>Pre-agglomeration:</b> ZVI:stabilizer = 1:4. Specific surface area = 20-30 m<sup>2</sup>/g. Mixing with PSS may enhance transportability of nZVI.</p>	Schrick et al., 2004; Hydutsky et al., 2007

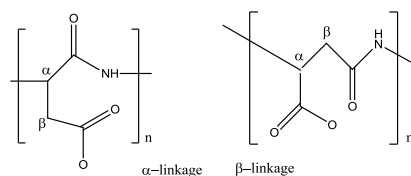
PAM Polyacrylamide. Nonionic polymer. M.W. = 5M. It binds with nZVI *via* hydrogen bonds with amine groups.



**Pre-agglomeration:** nZVI:stabilizer = 0.4. Primary particle size = 101 nm. Stabilization effectiveness: CMC > PAM > PSS > PAA

Cirtiu et al., 2011

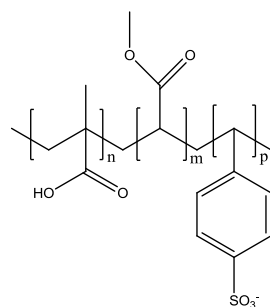
PAP Polyaspartate. Weak anionic polypeptide. M.W.= 2.5K or 10K.



**Post-agglomeration:** nZVI:stabilizer = 1:0.33. Coating thickness: ~40 nm for both PAP2.5K and PAP10K.

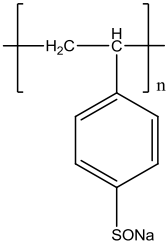
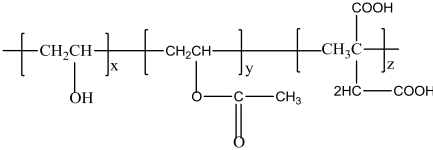
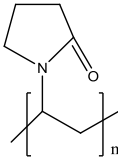
Phenrat et al., 2008a

PMAA-P MMA-PS Triblock copolymers: poly(methacrylic acid)-block-(methyl methacrylate or butyl methacrylate)-block-(styrenesulfonate) (PMAA-PMMA-PSS). It binds with nZVI via carboxylic groups of PMAA. The mixed coatings render nZVI amphiphilic.



**Post-agglomeration:** nZVI:stabilizer = 0.67. Hydrodynamic size = 178 ± 11nm. Compared with bare nZVI. The stabilization enhanced transport, but the stabilized nZVI decreased TCE dechlorination rate by a factor of 4.

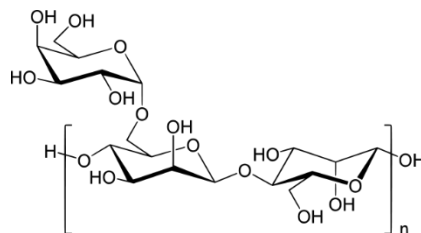
Saleh et al., 2005, 2007; Sirk et al., 2009

PSS	Polystyrene sulfonate. Strong anionic polyelectrolyte. M.W. = 70K or 1M. It binds with nZVI through sulfonate groups.		<p><b>Pre-agglomeration:</b> nZVI:stabilizer = 3. Primary particle size = 182 nm.</p> <p><b>Post-agglomeration:</b> nZVI:stabilizer = 1:0.33. Coating thickness = ~67 nm for PSS70K, and ~198 nm for PSS1M. Less effective than OMA.</p>	Cirtiu et al., 2011; Phenrat et al., 2008a
PV3A	Polyvinyl alcohol-co-vinyl acetate-co-itaconic acid. Netatively charged. M.W.=4300-4400. Food grade, nontoxic and biodegradable.		<p><b>Pre-agglomeration:</b> nZVI:stabilizer = 1:5 to 1:10. Primary particle size = 15 nm. A shift of the isoelectric point (IEP) from pH ~8.1 for bare ZVI to 4.5. Similar reactivity to that of bare ZVI towards TCE. Particles remain suspended after 6 months.</p>	Sun et al., 2007
PVP	Polyvinylpyrrolidone. Neutral. M.W. = 40K or 360K.		<p><b>Pre-agglomeration:</b> nZVI:stabilizer = 1:100. Primary particle size = 74.5 nm with PVP40K and 87.3 with PVP360K. Suspension remains stable for 1 – 10 h. Less effective than CMC.</p>	Sakulchaicharn et al., 2010

---

## Natural biopolymers

Guar gum Neutral polysaccharide. Also used for enhanced bioremediation. It binds with nZVI via the hydroxyl groups.

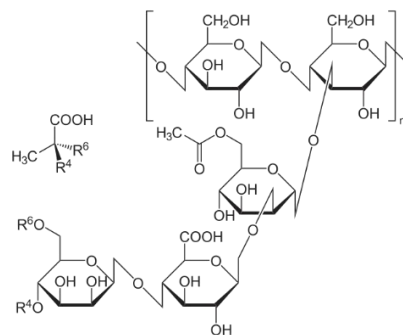


**Pre-agglomeration:** nZVI:stabilizer = 1:5. Mean particle size = 63.1 nm. Suspension remains stable for >48 h. Reactivity for TCE doubles that for bare ZVI. Higher dose (>1 g/L) of the stabilizer inhibits TCE degradation.

Sakulchaicharoen et al., 2010; Tiraferri et al., 2008, 2009

**Post-agglomeration:** nZVI:stabilizer = 0.9 to 2.7. Hydrodynamic size = 162 nm. More effective than starch. Very resistant to ionic strength.

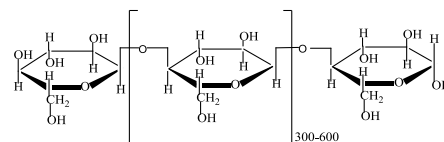
Xanthan gum Neutral polysaccharide. Beta-1,4-glycosidic bond linked.



**Post-agglomeration:** nZVI:stabilizer = 5 to 10. Suspension remains stable at ionic strength up to 12 mM. Stabilization is through a polymer network. Stabilized nZVI suspensions show a shear thinning behavior that is dependent on iron concentration.

Comba and Sethi 2009; Comba et al., 2011

Starch Neutral polysaccharide. nZVI-starch interactions and formation of intra-starch Fe clusters play a fundamental role in stabilizing nZVI.



**Pre-agglomeration:** nZVI:stabilizer = 0.05. Discrete nanoparticles attained with a mean size of 14.1 nm. Very reactive for TCE and PCBs degradation.

**Post-agglomeration:** nZVI:stabilizer = 0.38 to 1.15. Stabilization effectiveness is less than guar gum.

He and Zhao 2005;  
Tiraferrri et al., 2008

---

\* Mass ratio refers to the ratio of iron to stabilizer in a stabilized suspension.

## Figures

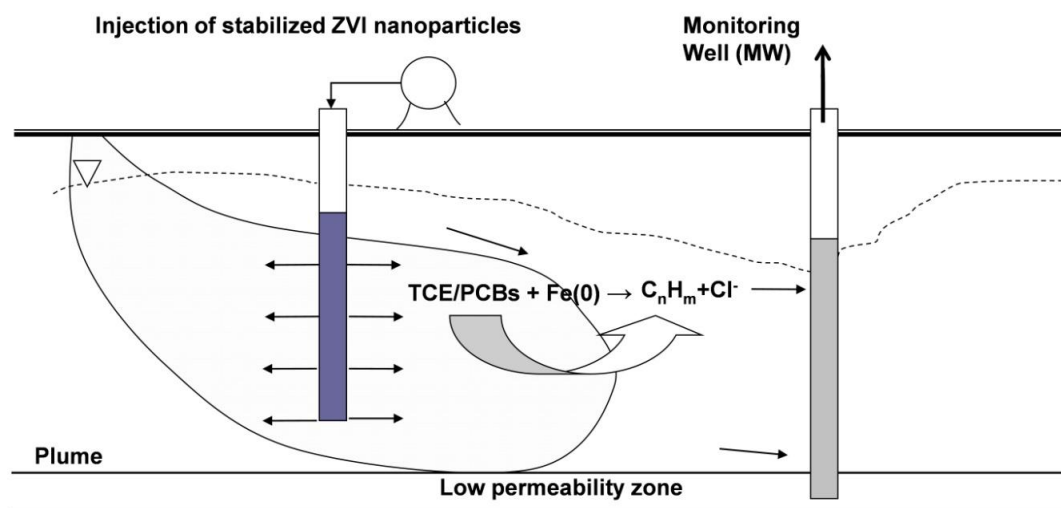


**Fig. 1.** A schematic of an *in situ*, proactive remediation technology for TCE/PCBs degradation using stabilized nZVI.



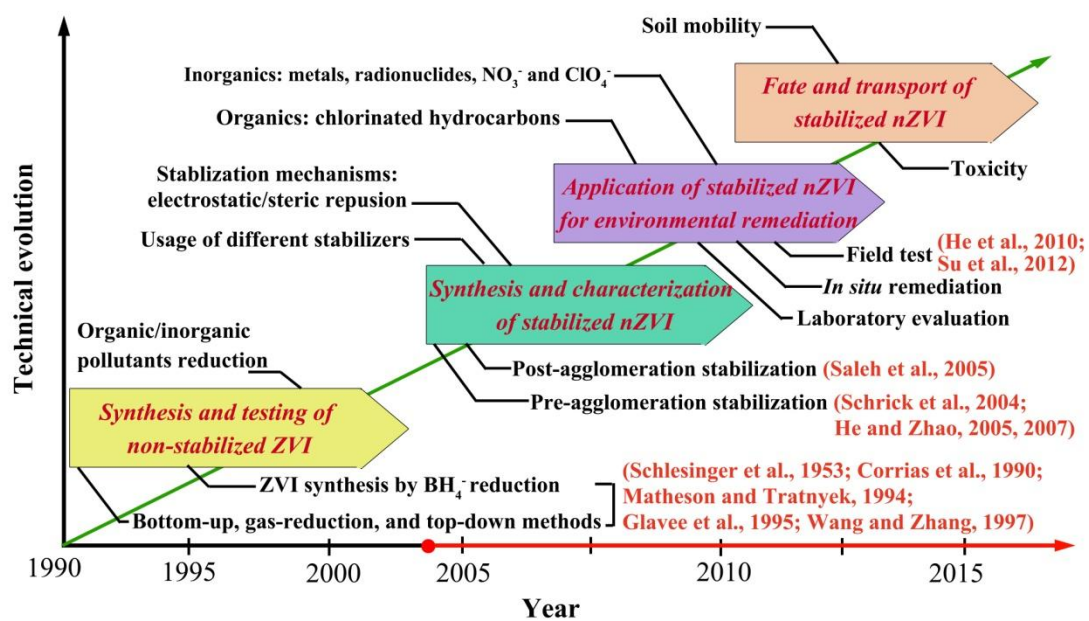
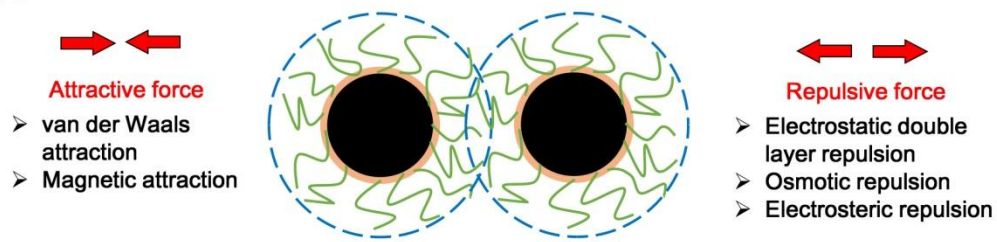


**Fig. 2.** Development and technical evolution of stabilized nZVI technologies.

(a) Surface modification stabilization



(b) Network stabilization

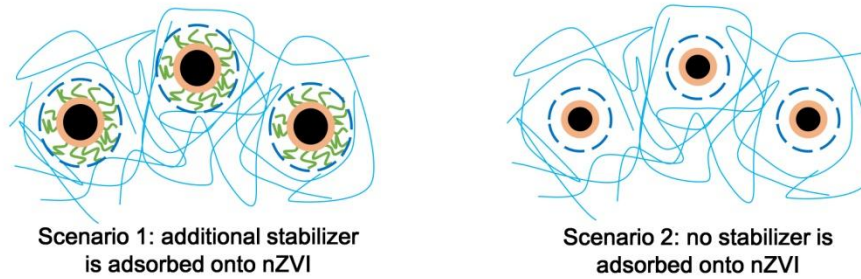


**Fig. 3.** Schematic representation of **(a)** surface modification stabilization (where surface coating facilitates particle repulsion), and **(b)** network stabilization (where a medium network is formed due to hydrogen bonding and polymer entanglements).

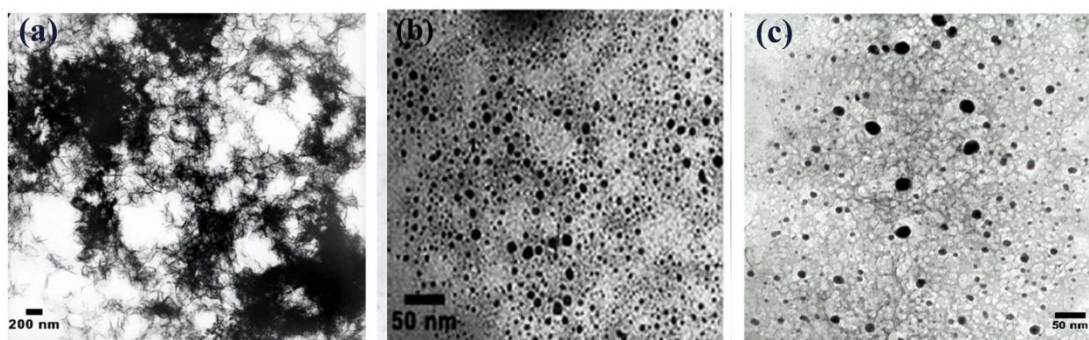


**Fig. 4.** TEM images of various Pd-Fe nanoparticles (Pd = 0.1 wt.% of Fe): **(a)** freshly prepared without a stabilizer, **(b)** freshly prepared with 0.2 wt.% of starch, **(c)** stabilized with 0.2 wt.% CMC and after 1-day of aging (stored in a sealed vial at 4°C). Particles were prepared through pre-agglomeration stabilization. (He and Zhao, 2005; 2007)

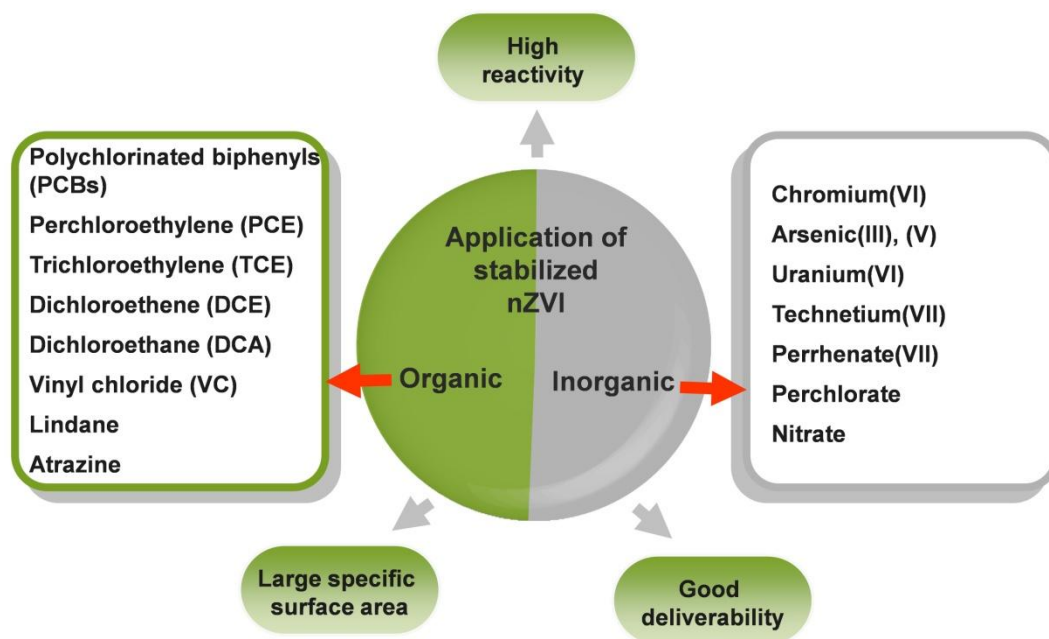


**Fig. 5.** Applications of stabilized nZVI for in situ remediation of contaminated soil and groundwater.

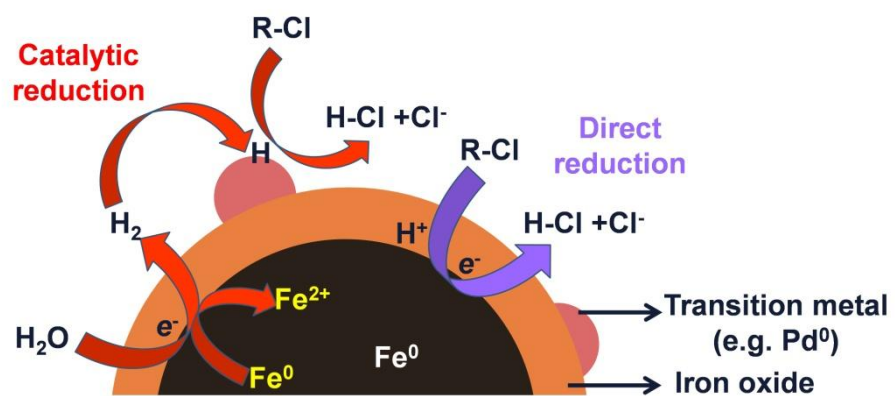


**Fig. 6.** Mechanisms of reductive dechlorination by nZVI with or without Pd catalyst.

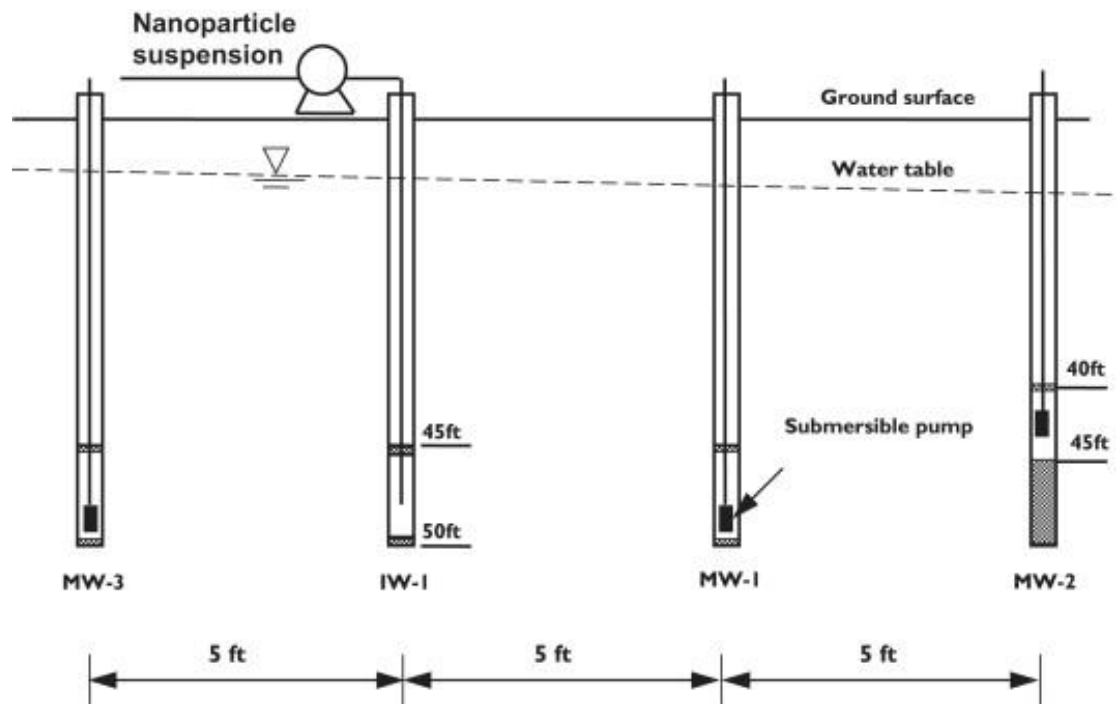


**Fig. 7.** A sectional view of the aquifer at the field testing site and schematic of the *in situ* injection of CMC-stabilized Fe-Pd nanoparticles (1 ft = 0.3048 m). (He et al., 2010)

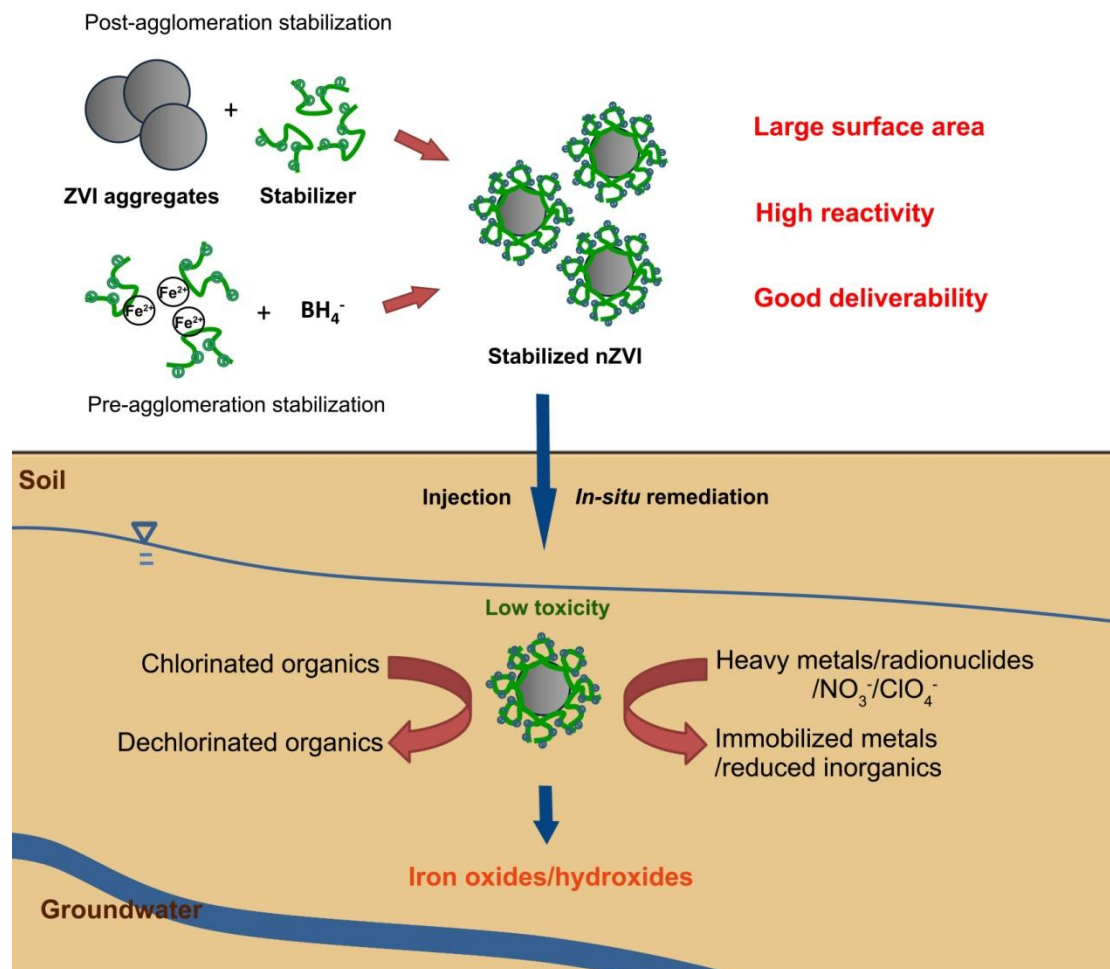


**Fig. 8.** Schematic diagram on synthesis, application, transport and fate of stabilized nZVI.